NTNU – Trondheim
Norwegian University of
Science and Technology

Optimization of Liquid-Rich Shale Wells

Asbjørn Holme

Petroleum Geoscience and Engineering
Submission date: June 2013
Supervisor: Curtis Hays Whitson, IPT

Norwegian University of Science and Technology
Department of Petroleum Engineering and Applied Geophysics

Abstract

The development of horizontal well technology and hydraulic fracturing have made production from shale and other low permeable rocks possible and revolutionized the oil and gas business. Shales produce typically with very low oil-gas ratios (high gas-oil ratios). For liquid-rich shales, it is shown that there is a significant difference between the initial solution oil-gas ratio and producing oil-gas ratio. In fact, what you produce at the surface is not the same as what you have in the reservoir. Shale wells produce with a low bottomhole pressure to maximize early gas rates and early rate of return. This comes with a drawback of reduced oil recovery. The combination of horizontal wells with hydraulically induced fractures and low permeability reduces the producing oil-gas ratio significantly compared to the initial in-solution oil-gas ratio. For liquid-rich shale gas condensate wells, the majority of the oil that is produced are produces as oil that is in solution in the gas phase. Little or no oil are produced as free oil. The fractures creates large volumes for the hydrocarbons to flow through and as the pressure drops below the dewpoint pressure near the wells, the build up of oil saturation is insufficient to become mobile oil in the near-fracture region. Most of the oil that condenses out of solution in the near-fracture region, are therefore unproduced resulting in a significant lower producing oil-gas ratio than the initial solution oil-gas ratio. The producing oil-gas ratio is directly linked to the producing bottomhole pressure. As the majority of the oil are produced as solution oil, the producing oil-gas ratio as a function of bottomhole pressure, will behave similar to the in solution oil-gas ratio of the fluid as a function of pressure. At higher pressures the gas contains more oil, and hence producing at a higher bottomhole pressure the gas will contain more oil as it is produced to the well resulting in a higher oil-gas ratio.

Producing at a bottomhole pressure equal to the dewpoint pressure eliminates the effect of lost oil in the near-well region and the producing oil-gas ratio are therefore equal to the initial solution oil-gas ratio. Producing at a higher bottomhole pressure will come at the cost of reduced gas production. As oil is a

more valuable commodity, the increased oil recovery at the expense of reduced gas recovery will in fact increase the net present value of the well. Optimizing the production in terms of finding the right bottomhole pressure may double the oil recovery of the well and increase the net present value of the revenues from the oil and gas sale by as much as 25 %. Even though the increased oil recovery come at the expense of reduced gas recovery, the gas is not lost. When the rates at producing at a high bottomhole pressure are not economical anymore, the bottomhole pressure can be lowered. The gas production then quickly catches up with the production coming from a well that have produced at a constant low bottomhole pressure. This thesis show that producing at a higher bottomhole pressure is the best economical choice for a wide range of cases. It is applicable for all gas condensate systems as well as near-critical and volatile oil systems. A significant low permeability as well as a significant degree of undersaturation (high initial pressure) are required for the method to be economical beneficial.

Sammendrag

Den teknologiske utviklingen av horisontale brønner og hydraulisk oppsprekning av reservoaret har gjort produksjon fra skifer og andre lav permeable bergarter mulig. Skiferbrønner produserer typisk med et lavt olje-gass forhold. For væskerike skifere, er det vist at det er en betydelig forskjell mellom olje-gass forholdet som er initiellt i løsning og det produserende olje-gass forholdet. Det du produserer på overflaten er ikke det samme som er i reservoaret. Skiferbrønner produserer med et lavt bunnhulstrykk for å maksimere gas ratene og tidlig avkastning. Dette kommer på bekostning av redusert oljeutvinning. Kombinasjonen av horisontale brønner med hydaulisk oppsprekning og lav permeabilitet reduserer det produserende olje-gass forholdet betraktling sammenlignet med det initielle olje-gass forholdet. For gasskondensat brønner, majoriteten av oljen blir produsert som olje som er i løsning i gassfasen. Lite eller ingen fri olje blir prousert. Sprekkene danner store strømingsvolum som hydrokarbonene må gjennom. Når trykket er mindre enn duggpunktstrykket nær brønnen, er oppbygningen av oljemetning for liten til at mobil oljemetning blir bygd opp. Mesteparten av oljen som kondenserer ut i nær-sprekk området blir dermed ikke produsert, som resulterer i et betydelig lavere olje-gass forhold enn det initielle olje-gass forholdet. Det produserende olje-gass forholdet har en direkte sammenheng med det produserende bunnhullstrykket. Ettersom mesteparten av oljen blir produsert som en del av gassen, vil det produserende olje-gass forholdet som en funksjon av bunnhullstrykk følge den samme trenden som løsnings olje-gass forholdet som en funksjon av trykk. Ved høyere trykk vil gassen inneholde mer olje, og ved å produsere ved et høyere trykk vil gassen inneholde mer olje når den blir produsert som resulterere i høyere olje-gass forhold.

Produksjon ved et bunnhullstrykk som er lik duggpunktstrykket vil hindre tap av olje i området nær brønnen, og det produserende olje-gass forholdet vil være likt the initielle olje-gass forholdet som finnes i løsning. Produksjon ved et høyere bunnhullstrykk vil komme på bekostning av en redusert gassproduksjon. Siden olje er en mer verdifull handelsvare vil den totale nåverdien av inntektene

fra brønnen øke. Optimisere produksjonen med tanke på å finne det optimale bunnhullstrykket kan dobble oljeutvinningen fra brønnen og øke nåverdien med 25 %. Selv om den økte oljeutvinningen kommer på bekostning av gassutvinngen, vil ikke gassen bli mistet for alltid. Når ratene ved et høyt bunnhullstrykk ikke lenger er økonomisk forsvarlig, bunnhullstrykket kan senkes. Gassproduksjonen tas da raskt opp igjen sammenlignet med en produskjon ved et konstant lavt bunnhullstrykk. Denne mastergraden viser at produksjon ved et høyere bunnhullstrykk er den beste økonomiske løsningen for et vidt spekter av tilfeller. Det er gjeldene for alle gass-kondensat systemer samt nær-kritiske og flyktige olje systemer. Lav permeabilitet og høyt initielt reservoar trykk er betingelser for at metoden er gjeldene.

Preface

This thesis is written as a final thesis in the five year Master of Science programme in petroleum engineering at the Norwegian University of Science and Technology (NTNU). The 4th year of the master study were spent as an exchange student at the University of Oklahoma, USA.

First I would like to thank my supervisor Curtis Hays Whitson for his advices and constructive feedbacks. Not only have he contributed to my master thesis, but his support and caring, technological and personally, throughout my master study have been a true inspiration and greatly appreciated. I would also like to thank Alexander Juell at NTNU/Pera for his help when it comes to the reservoir modelling and optimization part. A special thanks goes to family and friends. Finally I would like to thank my fellow students at the Department of Petroleum Engineering and Applied Geophysics and University of Oklahoma for making these five years a truly memorable experience with a great social and studying environment.

This thesis is dedicated to the memory of Johnny Solberg Anderson who tragically died in a work accident the 23th of April 2013.

Contents

List of Figures

List of Tables

Chapter 1

Introduction

Production from shale reservoirs have exploded in the recent years, creating an oil and gas boom in United States. Traditionally, shales have only been considered as a source rock and large scale production was unthinkable because of the extremely low permeability. Recent technological advances have proven that extraction of hydrocarbons from shales are economical. Long horizontal wells combined with massive hydraulic fractures gives a far greater reservoir exposure and wells are able to produce at economical high rates. This shale oil and gas boom have lead to increased activity in the oil and gas sector onshore United States creating thousands of jobs and helping the United States economy recover from the financial crisis. The shale gas may also help reduce greenhouse emissions (CO_2) as gas is a cleaner fossil fuel than coal and the cleaner natural gas products may also replace gasoline as fuel for cars.

The shale gas production have revolutionized the U.S. gas market, with the gas price dropping from around 15 dollars/million Btu to less than 2 dollars/million BTU in spring of 2012 [Henry Hub Natural Gas Spot Price, 2012] Figure 1.1 displays a map of the shale plays in the lower 48 states of the United States. The shale plays are located all over the United States and the potential of these plays are so big, that it might lead to United States becoming a net exporter of natural gas in the near future. The major shale plays are the Barnett, Eagleford, Haynesville, Woodford, Bakken and the Marcellus. Even though production from shale plays have so far been primarily in North America, it is expected to be expanded outside of North America. There are large resources in shale plays all over the world, particular in countries such as China, Canada and Argentina. Figure 1.2 is forecasting the natural gas production in the United States and

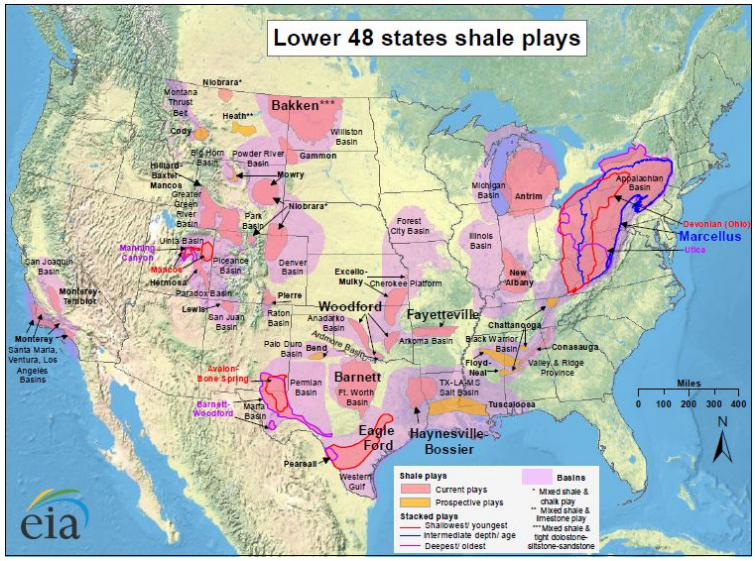

Figure 1.1: *Lower 48 states shale plays [U.S. Energy Information Administration]*

it is expected that shale gas in combination with tight gas will represent more than 50% of the total gas production in the United States. With the gas price currently at a very low level, the focus for the oil companies are now to go after liquid-rich shale. These are shale plays with a significant oil volumes in place in the form of oil and gas condensate. The Eagleford in Texas is a liquid-rich shale play producing at significantly higher oil-gas ratios than for example the Barnett and Marcellus shale. The Bakken shale located partly in North-Dakota, Montana and Canada is another shale liquid-rich shale play. Liquid-rich shales can be both oil or gas condensate, and is recognized by the higher oil rates (higher oil-gas ratio).

The best way to predict the performance of any oil and gas reservoir is with numerical reservoir simulation models. However, conventional techniques are not always applicable to unconventional reservoirs because of its complexity. The way the wells typically are completed, with hydraulic fractures, these fractures causes part of the near well area to be stimulated with a higher permeability than the matrix permeability. The stimulation causes therefore high initial rate by depleting the stimulated volume. Shale gas production are recognized with high initial ratse and fast decline which are typical of a transient performance where $\frac{dp}{dt} = f(t)$. unlike a typical pseudosteady performance $\frac{dp}{dt} = constant$. Con-

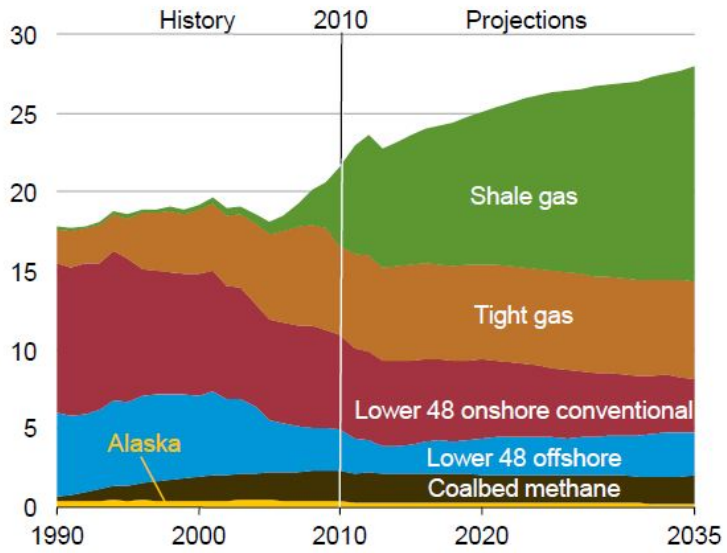

Figure 1.2: *US Gas Production 1990-2035 [U.S. Energy Information Administration, 2012]*

ventional reservoirs also have an early transient performance before the pressure transient has reached the outer boundary. Normally this transient period are a lot shorter than what is commonly observed in shale gas production and the dominante flow period is the pseudo-steady flow period where $\frac{dp}{dt} = constant$. The shale, and the fractures, can be modelled accurately using a very fine grid near the fractures to ensure that the transient effects are captured with commercially available simulators.

Chapter 2

Technical Background

2.1 Shale

Shale is a sedimentary rock defined as having more than 67 % clay minerals [Jackson, 1997], but the definitions are not clear and rocks with less than 67% clay minerals may still be categorized as a shale. Clay minerals have a grain size less than 0.002 mm according to the ISO-14688-1 scale. Typical shale minerals are kaolonite, montmorillonite and illite. Shales are characterized by the ability to break along parallel layers created by the orientation of the clay minerals when the rock was compacted. The clay minerals were typically sedimented at low energy environments. Organic material, planktons and algae, may deposit together with the clay minerals to later form kerogen. If a shale contains sufficient amount of kerogen it is a potential source rock or shale play. The total organic content (TOC), is a measurement of kerogen, oil and gas in a rock. The three different phases can be difficulty to distinguish, and the TOC is therefore used as a measurement of the hydrocarbon potential of the rock. When buried deep in the Earth's crust, the rock is heated and kerogen releases oil or natural gas depending on the conditions and the kerogen type. The released oil or natural gas gradually migrates upwards from the shale, the source rock.. Oil or natural gas will migrate all the way to surface, if they are not "trapped" and stored in conventional reservoirs. The migration process is a slow process and shales that are currently in the oil or gas window, can be characterized as both as source rock and a reservoir. When the shale is characterized as a reservoir the oil and gas can be extracted directly from the shale.

The key characteristic that distinguish shale plays from conventional plays are

the extremely low permeability. The very small grain sizes causes a large degree of compaction resulting in very small pores and pore throats (nano-size). This leads to an extremely low permeability. The extremely low permeability is the main reason why shale resources have often been thought of as unrecoverable and the reason why shales are classified as unconventional resources together with other types of resources such as hydrates and coalbed methane. Figure 2.1 shows the relationship between porosity and permeability for different types of rocks. The permeability ranges from 1000 mD (1D) for very permeable conventional reservoirs to 0.000001 mD (1nD) for very tight shale plays. Conventional reservoirs can have as much as 9 orders of magnitude higher permeability than shale reservoirs. Because of the low matrix permeability the recovery of oil and gas from shales must be done with new techniques to enhance the productivity of the wells. Stimulating areas of the reservoir with hydraulically induced fractures, enhances the permeability and enhances the productivity of each well.

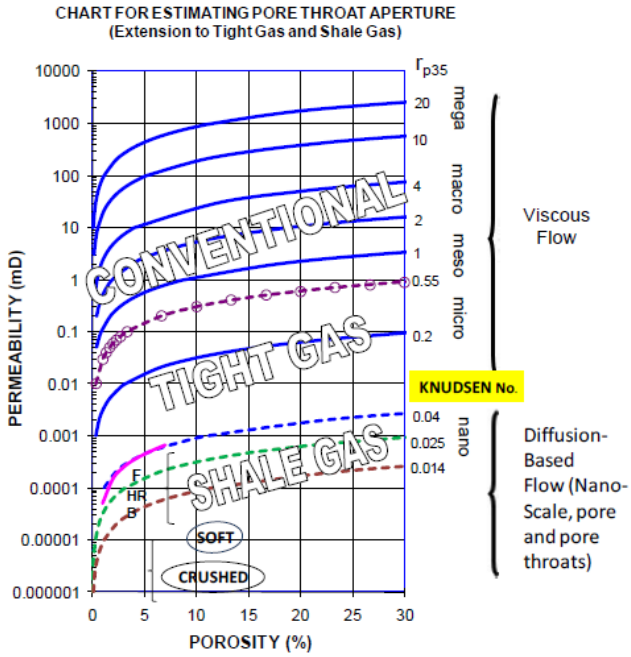

Figure 2.1: *Permeability versus porosity plot for shale to conventional reservoirs [Aguilera, 2010] where Samples from Fayetteville (F), Horn River (HR) and Barnett (B) are plotted together with correlations between porosity, permeability and pore throat size.*

2.2 Shale Plays

2.2.1 Shale Gas

First production from shale reservoirs started in the Barnett shale in the Forth Worth basin in north-Texas in the 80s [Bruner and Smosna, 2011]. Most of the knowledge about production comes from the Barnett shale, where the techniques of long horizontal wells and hydraulic fracturing were first tested. The techniques have been improved and perfected before transferred to other shale plays in different parts of onshore United States. The Barnett shale have natural fractured that provides flow paths for the hydrocarbons. The matrix permeability varies and are associated with a large degree of uncertainty and published values suggests matrix permeability in the range from millidarcy to nanodarcy. Porosity values are approximately 6% and water saturation are around 0.2-0.3, mostly bound to the matrix structure [Bruner and Smosna, 2011]. Jarvie et al. [2007] calculated the total organic content in the Barnett formation to be between 2 and 6 weight percent. The Barnett shale produces primarily methane, and the producing gas-oil ratio (R_p) in the core areas of the Barnett shale are above 100,000 scf/STB (r_p=10 stb/MMscf) [Tian and Ayers, 2010]. The Barnett shale is therefore characterized as a shale gas play. However, there are also parts of the Barnett formation that produces with significant lower gas-oil ratios and there is significant regional differences [Tian and Ayers, 2010]. Initial pressures in the Barnett shale are around 3-4000 psia, which makes it slightly overpressured with a pressure gradient around 0.5 psi/feet and a total drilling depth of 3-8000 ft. It is considered that the total gas in place in the Barnett formation may be as much as 30-40 Tcf.

The Marcellus shale formation in Pennsylvania and New York are similar to the Barnett shale. Producing mostly methane, it is also considered a gas play. Permeability for the Marcellus formation are also considered to be in the range from millidarcy to nanodarcy and porosity values are thought to be from 5 to 10%. Total gas saturation are around 0.6-0.8 and water saturation 0.4-0.8. No formation water is produced indicating immobile water or no free water present [Arthur et al., 2008]

2.2.2 Liquid Rich Shale

The Eagleford formation is another shale play located in Texas. Strictly speaking, the Eagleford is not a shale in geological terms, as it is more a carbonate than a shale. Still it is commonly know as a shale play as it shares many of the same

key characteristics as the other shale formations. The Eagleford have been the primary source rock for the Austin Chalk formation and production from the Eagleford did not attract attention before after the big developments in other shale plays such as the Barnett formation started. According to Wang and Liu [2011] the permeability in the Eagleford formation are from 40 to 1300 nano-darcies, matrix porosity from 5 to 14 percent and TOC values from 0.7 to 9.2 percent. Even though the permeabilities in the Eagleford formation are very low, it response well to stimulation by hydraulic fracturing. The low clay content and high carbonate content makes the formation brittle and easier to fracture [Eagleford Shale Geology]. The Eagleford formation differs from the Marcellus and Barnet formation by the high liquid yields. Eagleford produces large amount of heavier and intermediate components and less methane. Figure 2.2 shows a map over the Eagleford formation with drilled wells categorized as black oil, volatile oil, gas condensate or gas wells depending on the initial producing gas-oil ratios (R_p). As can be seen by figure 2.2, most of the wells in the Eagleford are

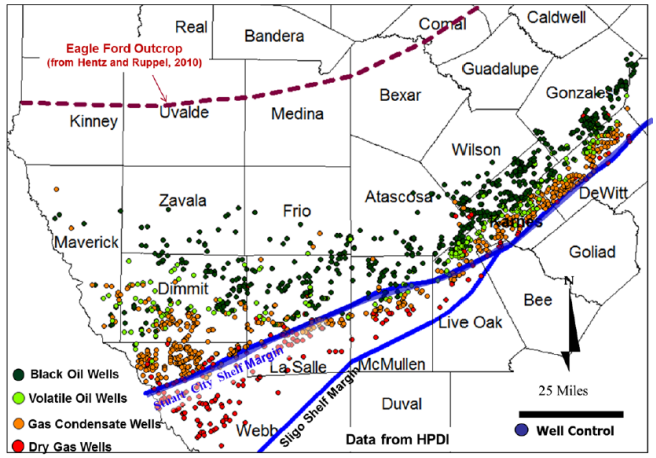

Figure 2.2: *Map of Eagleford shale play in Texas with all the wells drilled classified by the initial producing gas-oil ratio [Tian et al., 2013].*

either oil or gas condensate producers. Eagleford have therefore attracted large attention and the activity in the region is very high. However there are significant regional differences in the produced fluid types as discussed in Tian et al. [2013] For the wells characterized as "gas condensate" wells based on their initial gas-oil ratio, the producing gas-oil ratio are shown in figure 2.3. It is observed that there is a large spread in the producing gas-oil ratio for these wells, while the average producing gas-oil ratio stays at an almost constant level equal to 10,000 scf/stb

(r_p=100stb/MMscf).

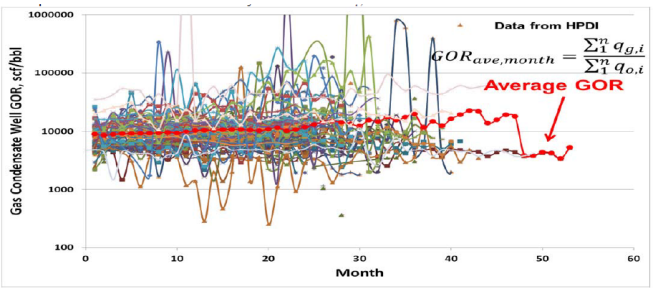

Figure 2.3: *Gas oil ratio for gas condensate wells in the Eagleford formation [Tian et al., 2013].*

2.3 Shale Production

2.3.1 Horizontal Wells and Hydraulically Fracturing

In conventional reservoirs vertical wells provide enough well deliverability, but in ultra-low permeability reservoirs the reservoir exposure must be increased to achieve the same well deliverability. The horizontal well starts off as a vertical well. At a certain distance above the target formation, directional drilling tools are used to build up an angle. When a desired angle (for horizontal wells 90°) is achieved, the drill string remains at this angle and starts drilling the lateral section. The lateral section of horizontal wells may be several thousand feet long. After the horizontal wells are drilled, the completion process starts. The wells are normally perforated in clusters. Each cluster also have a set of stages (perforations). Before the stimulation job, each cluster are separated with packers so only one cluster of the time are stimulated. Large amount of water (typically millions of gallons) are pumped with large trucks into the wellbore and into the perforations to fracture the formation. The pressure in the well must exceed the fracturing pressure of the formation. The fracturing pressure of the formation for a horizontal wells are given as [Fjær et al., 2008]:

$$p_w^{frac} = 3\sigma_H - \sigma_v - p_f + T_0 \tag{2.1}$$

Where p_w^{frac} is the fracture pressure (psia), σ_H the largest horziontal stress (psia), σ_v the vertical stress (psia), p_f the pore pressure (psia) and T_0 the tensile

strength of the formation (psia). The in-situ stresses are key parameters. The in-situ stresses not only determines the fracture pressure, but also determines the fracture orientation. The fractures will open perpendicular to the least principal stress (σ_h). In a normal tectonic situation the largest principal stress are the vertical stress. Horizontal wells should therefore be drilled along the direction of the least horizontal stress to create large vertical fractures perpendicular to the wellbore. To keep the fracutres open, large amount of proppants are pumped into the well. Proppants are often sands or glass beads that are pumped into the fractures and keeps the fractures from closing when the well pressure are reduced. Together with the water and proppants different additives are used to fracture the formation. Most common additives are gels that increases the viscosity of the water for better transportation of proppants into the fractures. Horizontal wells with hydraulic fractures increases the reservoir exposure tremendously and makes wells that would produce uneconomically rates with conventional completion techniques produce at economical rates. For further discussion of hydraulic fracturing see Fjær et al. [2008] and Gidley et al. [1989]

2.3.2 Flow in Shale Reservoirs

In conventional reservoirs vertical wells are drilled and the fluids flow radial towards the wellbore. For hydraulically fractured horizontal wells, radial flow ("pseudo-radial") are only observed once the well and fracture area are so small compared to the drainage area that the well is only seen as a point source. This will not happen during the lifetime of the well for reservoirs with low and ultra-low permeability.. Assuming the fractures are planar fractures extending a certain distance outwards from the well ($2x_f$) the majority of the flow will be perpendicular to the fracture. Wattenbarger et al. [1998] derived an equation by solving the diffusivity equation analytical for a one dimensional problem. This describes the linear one-dimensional flow in tight gas reservoirs towards a hydraulic fracture. In terms of dimensionless variables (see appendix 8) the rate equation for single phase oil can be written as:

$$\frac{1}{q_D} = \frac{\pi}{4} \frac{1}{\sum\limits_{n_{odd}}^{\infty} exp\left[-\frac{n^2\pi^2}{4} t_D\right]} \tag{2.2}$$

Where q_D is the dimensionless rate and t_D is the dimensionless time. Equation 2.2 have both short and long term approximations. The short term approximation for 2.2 for single phase oil are given as:

$$\frac{1}{q_o} = \frac{5.617\pi^{1.5} B_o}{h} \sqrt{\frac{\mu_o t}{k\phi c_t x_f^2}} \frac{1}{(p_i - p_{wf})} \tag{2.3}$$

Where:
q_o = oil rate, stb/d
B_o = oil formation volume factor, bbl/stb
h = the reservoir thickness, ft
μ_o = oil viscosity, cp
t = time, days
c_t = total compressibility, 1/psia
x_f = fracture half-length, ft
p_i = initial reservoir
p_{wf}= flowing bottomhole pressure, psia

And the long term approximation for equation 2.3 is:

$$\frac{1}{q_D} = \frac{\pi}{4}\left(\frac{y_e}{x_f}\right) exp\left[\frac{\pi^2}{4}\left(\frac{x_f}{ye}\right)^2 t_D\right] \tag{2.4}$$

Where y_e is the distance from the fracture to the outer boundary (ft). The short term approximation are appropriate to use for shale gas reservoirs, as the reservoirs flow period are predominantly infinite acting. A infinite acting flow period are characterized by the pressure change changing over time ($\frac{dp}{dt} = f(t)$) and no outer boundaries are reached. Equation 2.3 gives the flow rate proportional to the square root of time and are recognized by a half-slope when plotting the rate versus time on a log-log plot. The long term approximation are only valid for closed boundary (boundary dominated flow). Equation 2.3 can also be used for gas flow with good accuracy when substituting the pressures(p_i and p_{wf}), formation volume factor(B_o) and viscosity (μ_o) with pseudopressure function (m(p)) defined as:

$$m(p) = 2\int_{p_{ref}}^{p} \frac{p}{Z\mu} dp \tag{2.5}$$

The infinite acting linear flow for gas phase can then be written as:

$$\frac{1}{q_g} = \frac{56.33\pi^{1.5}T}{h}\sqrt{\frac{t}{k(\phi c_t \mu_g)_i x_f^2}}\frac{1}{(m(p_i) - m(p_{wf}))} \tag{2.6}$$

2.4 Economics

2.4.1 Oil and Gas Prices

Oil and gas prices are variables that changes over time. While the price of oil is more or less global, the price of gas is local due to its dependency of infrastructure such as pipelines. The shale gas revolution in the US have brought the gas price down in the US, while increased demand in Asia have brought the gas price up in Asia. At the time being the oil price for Western Texas Intermediate (US) is around 100 US dollar per barrel of oil, while the gas are sold for around 3 US dollar per Million British Thermal Unit (BTU) at the Henry Hub. A British Thermal Unit (BTU) is a unit for energy measurement and is defined as the heat required to heat 1 pound of water 1 degree Fahrenheit at a pressure of 1 atmosphere. A more common measurement when reporting gas production are thousand standard cubic feet (Mscf). Conversion between cubic feet of gas to BTU depends on the quality of the natural gas and therefore varies. The average heat content of 1 Mscf is roughly equal to 1.023 MMBTU [U.S. Energy Information Administration, 2013] which gives the price of gas ≈3 US dollar per Mscf. Converting from barrels of crude oil to BTU causes the same difficulties as with natural gas as 1 bbl of oil is not the same barrel of oil everywhere at any time. The US Energy Information Administration operates with a conversion of 1 bbl=5.8 MMBTU. For a oil price of 100 USD/bbl, the same price in terms of BTU are around 17 USD/MMBTU. That is 5.75 times more than for 1 MMBTU of natural gas! This is a good incentive to focus on increased oil recovery as it shows that oil is a more valuable commodity than gas.

2.4.2 Net Present Value

Calculating the net present value of a series of cash flows is a common method in finance to convert future cash flows to present value. As cash flows you have today are seen as more valuable than cash flows in the future, the future cash flows are discounted to account for inflation and expected return on present day cash flow. This is done with a discount factor which takes into account these factors. The discount factor used for the calculations in this thesis is set to 10%. For this thesis the cash flows are discounted annually, meaning that the cash flows from day 1 to 365 are discounted at the end of year 1 and so forth. The NPV are given by equation 2.7.

$$NPV = \sum_{t=0}^{N} \frac{CF}{(1+d_f)^t} \tag{2.7}$$

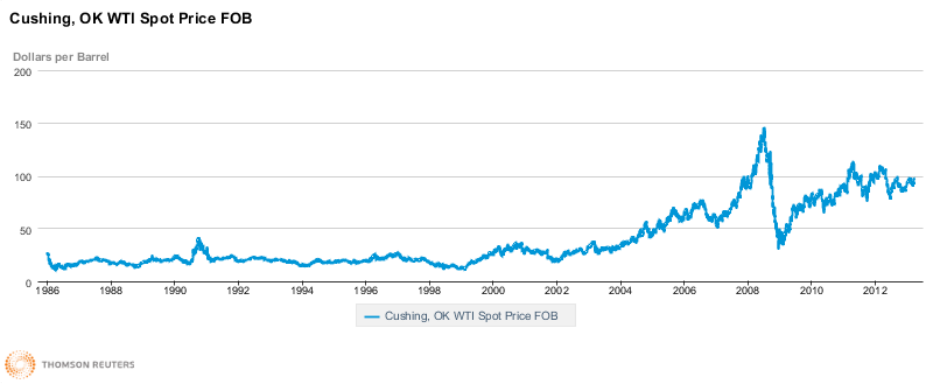

(a) WTI Oil Price

(b) Henry Hub Natural Gas Spot Price

Figure 2.4: *Oil and gas Prices in the US*

Where CF denotes future cash flow, d_f the interest rate and t is time. R can also be expressed as continuous rate of cashflow, r(t). The sum in equation 2.7 can then be expressed as an integral. For the purpose of this thesis the continuous cashflow can be rewritten in terms of flow rates, oil and gas prices minus the costs. Instead of using the oil rate, the oil rate can be expressed as the product of the producing oil-gas ratio and the gas rate. Equation 2.7 can then be rewritten as:

$$NPV = \int_0^t \left(\frac{G_p q_g(t) + 10^{-3} O_p r_p q_g(t) - C(t)}{(1+d_f)^t} \right) dt \tag{2.8}$$

Where G_p is the gas price (USD/Mscf), q_g is the gas rate (Mscf/d), O_p is the oil price (USD/stb), r_p is the producing oil-gas ratio (stb/MMscf) and C is the cost term (USD).

The cost term includes both operating costs and the initial drilling costs. The costs associated with drilling and completion operation are by far the highest costs for onshore extraction of hydrocarbons from shale plays. The net present value calculations performed in chapter 6, are looking at optimizing the bottomhole pressure to increase the net present value. The initial drilling and completion costs are assumed to be independent of producing bottomhole pressure, and the difference in operating costs for changes in the bottomhole pressure are assumed to be small and the cost term is therefore ignored in this thesis. Only the revenues generated from oil and gas sales are considered in chapter 6. Equation 2.8 reduces then to:

$$NPV = \int_0^t \left(\frac{G_p q_g(t) + O_p r_p q_g(t)}{(1+d_f)^t} \right) dt \tag{2.9}$$

2.5 Reservoir Fluids

2.5.1 PVT Properties

The reservoir fluid, oil or gas, may be very different from reservoir to reservoir. Based on the fluid composition the properties of the fluid varies. The reservoir fluid can be described graphically with phase diagrams. A phase diagram displays the relationship between pressure and temperature (P-T diagram), pressure and volume (P-V diagram) or temperature and volume (T-V). For a single component system, the system will be at different phases, solid, liquid and vapor, for different pressures and temperatures. The different phases are separated by solid-vapor, solid-liquid(melting curve) and liquid-vapor(vapor pressure curve) lines. The liquid-vapor line ends in a critical point. Beyond the critical point the liquid and vapor phase are indistinguishable. For systems with two or more components the vapor pressure curves of the system will lay between the vapor pressure curves of the single components. Instead of a single curve, a phase envelope can be drawn. Inside the phase envelope the two phases, vapor and liquid, coexists in equilibrium. The bordering curves of the phase envelopes are called bubblepoint line, where the first bubbles of gas starts coming out of the liquid phase and dew point line, where the first drops of liquids starts falling out of the vapor phase. The point with the maximum temperature and pressure on the phase envelope are known as cricondentherm and cricondenbar respectively.

Gas-Oil Ratio
An important relationship is the gas-oil ratio(GOR), which determines the ratio of surface gas to surface oil. This relationship is important to determine the richness of the fluid and whether the fluid is classified as a "heavy oil", "volatile oil", "gas condensate", "wet gas" or "dry gas". Monitoring the gas-oil ratio over time can also determine whether or not the reservoir pressure is below a bubble-point or dew-point. Above either a bubble-point or dew-point the gas-oil ratio are constant.

$$R = \frac{V_{\bar{g}}}{V_{\bar{o}}} \tag{2.10}$$

The fluids at the surface may be different from the fluids in the reservoir for example if the heavier components are left in the reservoir while all the lighter ones are produced to surface. It is therefore common to distinguish between solution gas-oil ratio, R_s, and the producing gas-oil ratio, R_p. The gas-oil ratio

may also change over time. The initial solution gas-oil ratio, R_{si} are given as:

$$R_{si} = \frac{IGIP}{IOIP} \tag{2.11}$$

Where IGIP are the initial gas in place in scf and IOIP are the initial oil in place in stb, giving R_{si} the units of scf/stb. The producing gas-oil ratio are given as:

$$R_p = \frac{q_g}{q_o} \tag{2.12}$$

Where q_g are the surface gas rate in scf and q_o the surface oil rate in stb, giving R_p the same units as R_{si}, scf/stb.

Oil-Gas Ratio
For gas condensates and oil reservoirs with high gas-oil ratios it is more convenient to use the inverse relationship, oil-gas ratio(r), as the oil volume relative to gas is so small that the gas-oil ratios values gets very high. The OGR are defined as:

$$r = \frac{V_{\bar{o}}}{V_{\bar{g}}} = \frac{1}{R} \tag{2.13}$$

With the units of $V_{\bar{o}}$ given in stb and $V_{\bar{g}}$ in MMscf instead of scf. The solution OGR and producing OGR are the inverse of solution GOR and producing GOR respectively.

2.5.2 Reservoir Fluid Systems

Dry Gas
A dry gas is a gas that produces no liquids at the surface. The temperature through the entire process from reservoir to stock tank is greater than the cricondentherm. The gas-oil ratio is infinite and no liquid are present.

Wet Gas
Wet gas produces some liquid at the surface. The reservoir temperature is beyond the cricondentherm, but as the gas is separated to surface conditions some liquids condensates as the surface conditions are inside the two-phase envelope. The stock tank gravity of the oil can be up to 70° API and the oil is normally water-like in colour. [McCain Jr., 1994]

Gas Condensate
Reservoirs that have reservoir temperature between the critical temperature and

the cricondentherm are defined as retrograde gas-condensate reservoirs. The reservoir fluid at reservoir conditions are gas. When the reservoir is depleted the reservoir pressure drops and the reservoir fluids enters the two-phase region. Such gas reservoirs produces a significant amount of condensate at the surface and exhibits gas-oil ratios between 3,000 and 150,000 scf/STB (oil-gas ratios from 5 to 350 STB/MMscf) [Whitson and Brule, 2000] and stock tank gravities between 40 and 60° API. The colour may vary, but is often brighter than volatile oil and typically yellow, white or light-brown. A typical C_{7+} content is less than 12.5 mol %. Some of the oil in a retrograde gas condensate will re-vaporize again at low pressures.

Volatile Oil
A reservoir fluid is defined as an oil, as long as the reservoir temperature is less than the critical temperature of the fluid. A volatile oil is an oil with relative high gas-oil ratios, from 1,000 to 3,000 scf/STB. Stock tank gravity of the oil is often between 35 to 50 ° API and the oil is normally yellow to brown in colour. Normally the solution gas of a volatile oil is a rich gas containing significant oil volumes. It is therefore important to remember to include r_s of the solution gas to calculate the total oil recovery. In terms of gas-oil ratio and surface properties, a volatile oil is fairly similar to both a gas condensate and black oil. A volatile oil may overlap with these two other reservoir fluids and may be hard to distinguish from each other based on surface properties only.

Black Oil
A black oil has a reservoir temperature less than the critical temperature and normally further away from the critical temperature than a volatile oil. Black oils have lower gas-oil ratios, typically less than 1,000 scf/STB and stock tank gravity less than 35 ° API. The colour is brown or black corresponding with a high C_{7+} content. Unlike the volatile oil, the solution gas is dry and recondensation of the gas does not contribute significantly to the overall oil recovery.

Chapter 3

Model Description

The work in this thesis is done using an integrated modelling software, Pipe-It [Petrostreamz, 2013]. Pipe-It enables several different programs to be launched at the same time and linking input and output data from the different programs together. This simplifies optimization problems significantly, as parameters can be optimized in all parts of the problem at the same time, using the built in optimization techniques. Most of the modelling work in this thesis are performed with the use of a Pipe-It template created by Aleksander Juell at Pera. The template consists of three main parts; a reservoir simulation part, a history matching part and a design optimization part.

Reservoir Simulation Model
The simulation work of this thesis is done with the use of the commercial numerical reservoir simulator software SENSOR [Coats Engineering, Inc., 2013]. Other commercially available simulator could also have been used in this study.

History Matching
The history matching part of the template enables actual observed data to be compared with simulator output. Optimizing sum of squares to get a best fit makes the process of history matching an efficient process. In this thesis, no history matching is performed.

Optimization
The optimization part of the Pipe-It project is greatly utilized in this thesis. The produced rates from the reservoir simulator are transferred into values for given oil and gas prices. The net present value from the produced oil and gas rates are then calculated. Using the optimization wizard enables an easy set up to run a

wide range of different cases and compare the net present values of these cases to optimize the asset.

3.1 Reservoir Simulation Model Description

The reservoir simulation model is based upon various data from shale plays onshore United States. An accurate simulator model is essential to get reliable results. The reservoir is assumed to be homogeneous and the hydraulic fractures are assumed to be uniformly distributed along the wellbore. The fracture is also assumed to be a planar fracture penetrating the entire thickness of the shale reservoir. This is somewhat a rough simplification of the real situation, but is thought to give reliable results. In reality micro-seismic mapping shows that the fractures are instead complex fracture networks, where the stimulation have reopened closed natural fractures. Creating a model with sufficient grid refinement for a complex fracture network is difficult and requires a large number of grid cells for each matrix block surrounded by fractures. The depletion of the matrix blocks depleting into the fractures can be modelled with the use of super-positioning of a few dual porosity grid cells [Holme, 2012]. Assuming each matrix block behave independently of each other the total well performance can be modelled. Whitson and Sunjerga [2012] argues that the difference in a 2D planar fracture model and a fracture network model is small. In this thesis only a planar fracture model is considered. It is also unlikely that all the clusters in every stage take the same treatment and produce fractures with equal length and properties, but if average properties are applied to the fractures a uniform distribution of the fractures are assumed to be decently accurate. Because of symmetry across the wellbore, only one half of the fracture have to be modelled. Since the fractures are assumed to behave independently of each other and equally only one fracture is modelled. The total well performance is then the product of the number of fractures and the performance from one fracture. Both a simplified 1D model, which ignores drainage beyond the fracture tip, and a more accurate 2D model is used in this thesis. The horizontal well is located along the x-direction and the fracture is located perpendicular to the wellbore, in the y-direction. When the well is stimulated, water at high pressure are pumped into the well to create hydraulic fractures. Some of this water are flowed back immediately, but some of it are never recovered to the surface. Most likely some of the rock itself are changed, and are able to store the water at only high pressures and are therefore kept in the formations. High water rates are also common in the time after stimulation. This is however ignored in this thesis, even though it may be simulated with commercially simulators injecting an amount of water before production and having stress dependent transmissibilities.

3.1.1 Grid dimensions

To model the fracture accurate and capture the transient effects a fine grid is applied with increasing grid sizing outwards. A total of 79 grid cells in the x-direction, 39 grid cells on each side of the fracture is used. In the y-direction 50 grid blocks are used, with increasing size outwards from the fracture tip. 30 grid blocks along the fracture and 20 grid blocks beyond the fracture tip. See appendix 8 for table with grid dimension. The lateral section of the wellbore is set to 5807 ft with 27 fractures. A common well spacing in the Marcellus shale play is 160 [Bruner and Smosna, 2011] acres while in the Eagle Ford and Barnett shale formations a closer well spacing is common. In this model the well spacing is set to 100 acres. According to Eagle Ford Information [2013] the average depth in the Eagle Ford formation are 250 feet and is the basis of the thickness of the reservoir simulator model. If insufficient grid blocks are applied, non-converged numerical simulations are seen, with typical oscillating producing oil-gas ratio (fig. 3.1). While the gas rate remains similar for most grid configuration, insufficient amount of grid blocks causes large fluctuations in the oil saturation near the fracture resulting in a oscillating oil rate resulting in an oscillating oil-gas ratio (this also affects the gas rate to some extent, but have an significantly less impact on the gas rate than on the oil rate).

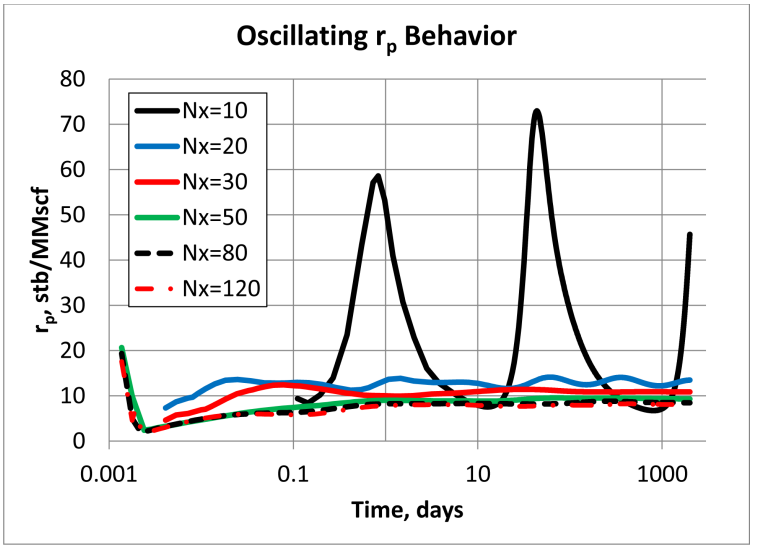

Figure 3.1: *Producing oil-gas ratio behaviour for different number of grid cells in the x-direction for 1D model.*

3.1.2 Reservoir Fluid

The reservoir fluid composition is created by first defining an oil with separator oil-gas ratio of 300 stb/MMscf, stock tank oil gravity of 48° API and surface gas specific gas gravity of 0.79. The composition is made up of H_2S, CO_2, N_2 and C_1 to C_{26+}. PhazeComp is used to find a converged composition that gives the specified oil-gas ratio and surface gravities using the Soave-Redlich-Kwong equation of state. Blackoil tables are then constructed internally in SENSOR by converting the equation of state to blackoil properties using the Whitson-Torp method. To elevate the saturation pressure, equilibrium gas (gas composition at the bubble point of the original oil) is added. If the equilibrium gas was not added, the gas phase would be limited to $r_{si} < 41$ stb/MMscf for the gas phase and for the oil phase $r_{si} > 325$ stb/MMscf. The added equilibrium gas elevates the critical point to 3909.4 psia at reservoir temperature (135F). An essential parameter in this thesis is the solution oil-gas ratio as a function of pressure which is displayed in figure 3.2. For the gas phase the solution oil-gas ratio ranges from 138 stb/MMscf at the critical point to 1.34 stb/MMscf at 800 psia. The critical fluid is 100 times richer than at 800 psia! The base case gas condensate simulator model is initialized with r_{si} of 100 stb/MMscf (R_{si} of 10,000 scf/stb) corresponding to a dewpoint pressure of 3798.5 psia. .

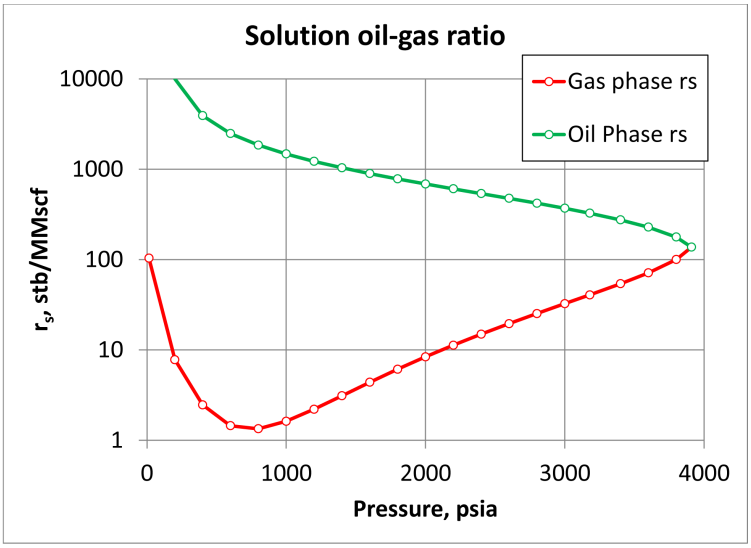

Figure 3.2: *Solution oil-gas ratio of reservoir fluid. Oil phase (green) and gas phase (red).*

A compositional model is also used in section 5 to calculate k_{rg}/k_{ro} relationships. The components used in the compositional model are the same componenets described above where the composition and EOS data for the reservoir fluid with $r_{si} \approx 100$ stb/MMscf and $p_d \approx 3800$ psia are shown in appendix 8. The difference between the blackoil model and compositional are small (figure 3.3). The blackoil model is therefore assumed to be accurate enough and is significantly faster to run than the larger compositional model. The black-oil model is used for all simulations except in chapter 5.

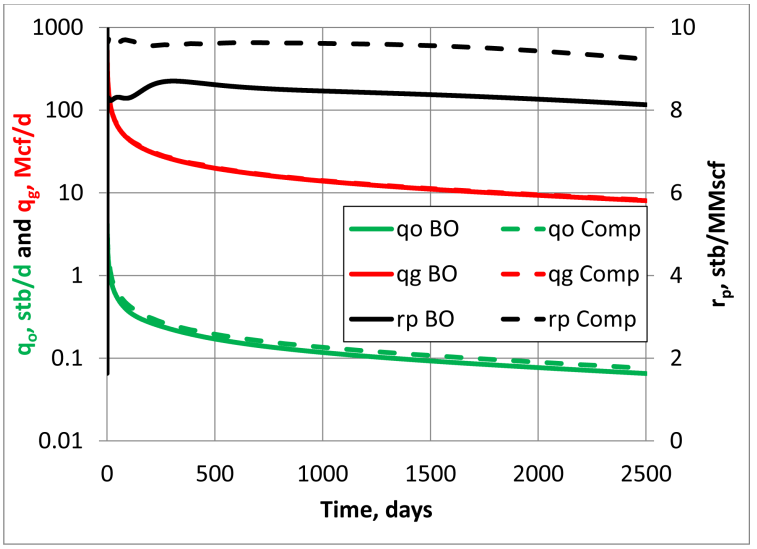

Figure 3.3: *Oil rates (green), gas rates (red) and producing oil-gas ratio (black) for black oil (solid lines) and compositional model (dotted lines).*

3.1.3 Rock Properties

Tight reservoirs, such as shale reservoirs, are recognised with low porosities and very low permeabilities. The literature [Aguilera, 2013, Walls et al., 2011] shows a wide range of varying rock permeability and porosity for shale systems. From a few nano-darcies (nD) to milli-darcies (mD). A reasonable value used in this thesis for permeability are 1e-4 mD and for porosity 0.05. The fracture conductivity, defined as the product of fracture width and fracture permeability, are set to 1000 mD-ft. This is equivalent of a infinite conductive fracture where the pressure drop

in the fracture can be neglected. The fracture half-length (x_f) is set to 150ft and the connate water saturation is set to 0.2.

3.1.4 Relative Permeability

The relative permeability of a fluid is defined as the ratio of its effective permeability to the absolute permeability of the reservoir rock.

$$k_{ri} = \frac{k_i}{k} \tag{3.1}$$

Where k_{ri} is the relative permeability of phase i, k_i is the effective permeability of phase i (mD) and k is the absolute permeability of the reservoir rock (mD). The relative permeability is a function of the saturation of the different phases. How the relative permeability changes with saturation can be determined experimentally with special core analysis (SCAL) in a laboratory or it can be estimated using correlations. Relative permeability from lab analyses is normally entered as table format in reservoir simulators and the reservoir simulator interpolates between the data points to get the relative permeability as a function of saturation. Relative permeabilities given as correlations are entered as equations, and relative permeability for any saturation can be calculated using the correlation. In this thesis, the relative permeability is estimated using Corey power-law relative permeability correlations, implemented in SENSOR with the use of the KRANALYTICAL keyword. In this case only oil and gas relative permeability are of interest as only connate water saturation is present for the entire simulation period. The relative permeability correlations for oil and gas respectively are given as [Coats Engineering, Inc.]:

$$k_{rog} = k_{ro}(S_{wc}) \left(\frac{1 - S_{org} - S_{wc} - S_g}{1 - S_{org} - S_{wc}} \right)^{n_{og}} \tag{3.2}$$

$$k_{rg} = k_{rg}(S_{org}, S_{wc}) \left(\frac{S_g - S_{gc}}{1 - S_{org} - S_{wc} - S_{gc}} \right)^{n_g} \tag{3.3}$$

Where:
k_{rog}= oil relative permeability to gas
k_{rg}= gas relative permeabilit
$k_{rog}(S_{wc})$=oil relative permeability at connate water saturation
$k_{rg}(S_{or}, S_{wc})$=gas relative permeability at residual oil saturation and connate water saturation
S_{wc}=connate water satuartion
S_{org}=residual oil saturation to gas

S_g=gas saturation
S_{gc}=critical gas saturation
n_{og}=oil relative permeability exponent
n_g=gas relative permeability exponent

In this thesis the connate water saturation and residual oil saturation to water and gas is both set to 0.2. The critical gas saturation is set to 0.1 and the relative permeability end points ($k_{rog}(S_{wc})$ and $k_{rg}(S_{or}, S_{wc})$) is set to 1. The base case relative permeability exponents of oil and gas is set to 2. Inside the fractures, straight line (n=1) relative permeability are used with the same end points as the matrix.

3.1.5 Flowing Bottomhole Pressure and Separator Conditions

The flowing bottomhole pressure (p_{wf}) for the base case reservoir model is set to 1000 psia. The bottomhole pressure are the primary optimization variable discussed in chapter 6. The separator is a two stage separator with the first separator conditions at a pressure of 440 psia and temperature of 110 Fahrenheit. The second stage separator conditions are 14.7 psia and 60 degrees F (standard conditions).

3.2 1D Model

A 1D model is a simplified model where only the fracture is modelled and everything beyond the fracture tip is ignored. This neglects the different flow regime at the fracture tip. The flow in the reservoir is one dimensional, linear and symmetrical towards the fracture. The 1D model is similar to the 2D model in all other aspects. A 2D image of the 1D model can be seen in figure 3.4 displaying the pressure distribution after 365 days of production. It should be noted that in the one dimensional case, there is only one grid cell in the y-direction with length equal to the fracture half length (150 ft) and the grid dimensions in the x-direction can be seen in appendix 8 table 5. Oil and gas production rates as well as the producing oil-gas ratio (r_p) of the 1D base case model can be seen in figure 3.5

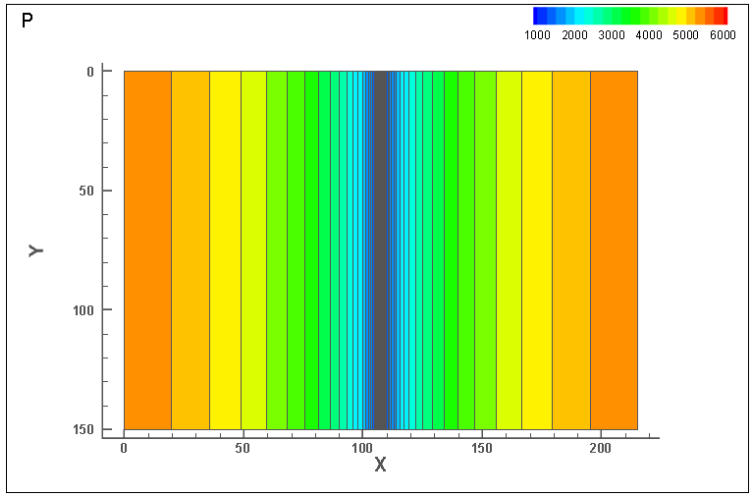

Figure 3.4: *Close up of 1D model at 365 days*

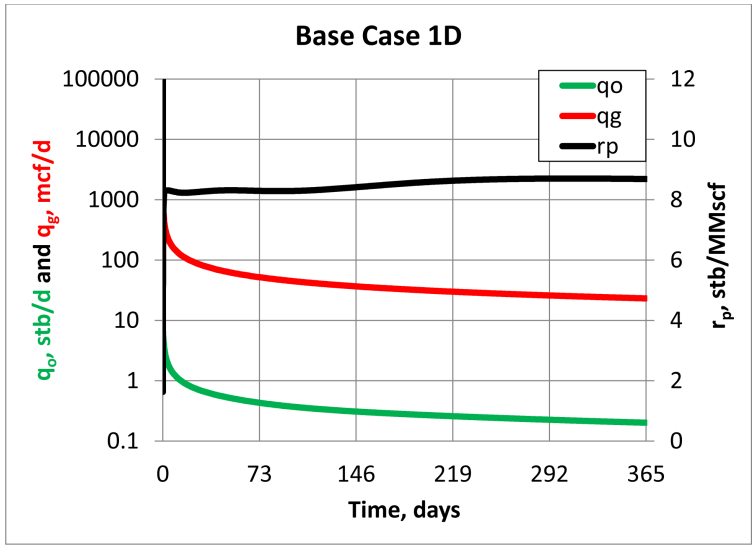

Figure 3.5: *Oil rates (green), gas rates (red) and producing oil-gas ratio (black) for the 1D base case model.*

3.3 Fracture Tip Effects and 2D Model

The end of the planar fracture will act as a point source with drainage beyond the tip. The drainage area will be a semi-circle, with the fracture tip in the origin and the flow will be radial towards the tip unlike the linear flow perpendicular to the fracture (fig. 3.6). Very fine Cartesian grid needs to be applied near the fracture to be able to capture this effect. In addition to a different flow regime, the drainage area increases. The pressure distribution of the 2D grid after 365 days of simulation can be seen in figure 3.7. The oil rate, gas rate and producing oil-gas ratio are plotted in figure 3.8. Note that the producing oil-gas ratio is generally higher for the 2D than for the 1D case and is increasing with time due. The reasons for the higher producing oil-gas ratio and the general increasing producing oil-gas ratio with time will be further discussed in chapter 5.3. The 2D model is thought to be more accurate since it also includes drainage beyond the fracture tip, and is the model used in chapter 6.

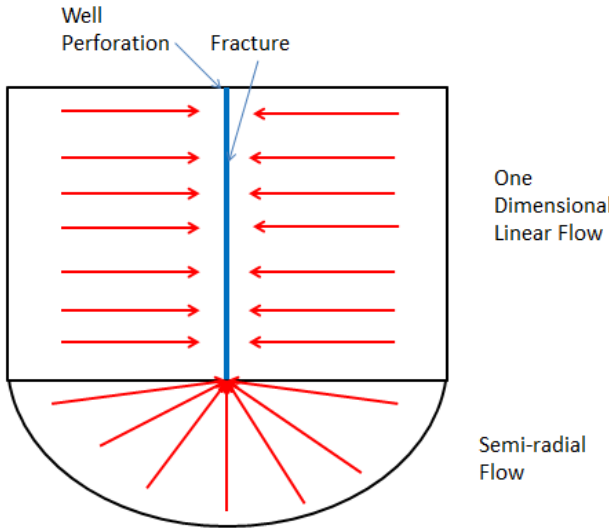

Figure 3.6: *Sketch of flow paths for 2D flow into fracture*

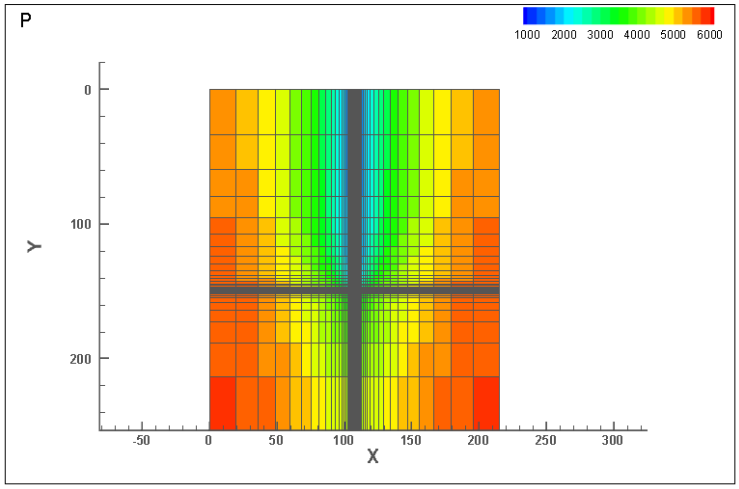

Figure 3.7: *Close up of the 2D model at 365 days*

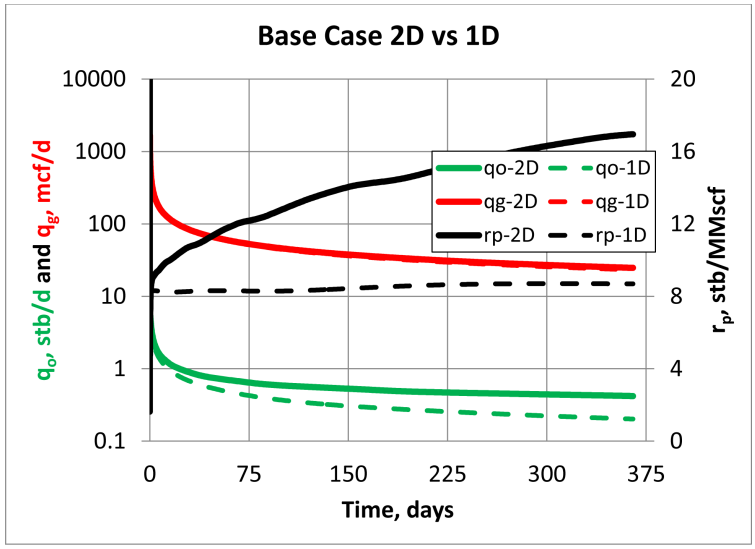

Figure 3.8: *Oil rate (green), gas rate (red) and producing oil-gas ratio (black) for 2D (solid lines) and 1D (dotted lines) simulation models.*

Chapter 4

Producing Oil-Gas Ratio

The producing oil-gas ratio is an important characteristic for liquid rich shale wells. It determines the richness of the produced fluids. High oil-gas ratio means more valuable oil, and low oil-gas ratio means more gas. Particularly interesting for liquid rich shale gas is that what you produce at the surface is generally not the same as what you have in the reservoir [Whitson and Sunjerga, 2012]. The producing oil-gas ratio may be significantly less than the in solution oil-gas ratio. These shale wells are typically drilled as long horizontal wells and stimulated with hydraulic fractures and producing with a very high drawdown (low p_{wf}) to maximize the gas rate. The high drawdown, combined with the large wellbore area (well+fractures), causes a large portion of the oil is lost in the near-wellbore (fracture) region. Conventional reservoirs on the other hand may produce with a oil-gas ratio equal to the in solution oil-gas ratio for a significant amount of time. The oil rate can be expressed as the sum of the oil being produced as solution oil ($r_s(p_{wf})$) and oil that flows freely in the reservoir:

$$q_{o-total} = q_{o-free} + q_g r_s(p_{wf}) \tag{4.1}$$

For many liquid rich shale gas reservoirs the producing oil loss is as high as a factor of 2 to 50 and the producing oil-gas ratio is equal to the solution oil-gas ratio at the flowing bottomhole pressure [Whitson and Sunjerga, 2012]! No free oil is produced. For some undersaturated ($p_R > p_d$) gas condensate reservoirs, the producing oil-gas ratio is slightly higher than $r_s(p_{wf})$ indicating that some free oil is produced, but still a significant portion is "lost" in the reservoir. The producing oil-gas ratio appears to be dependent of a number of factors with main factors being producing bottomhole pressure (p_{wf}), degree of undersaturation (initial reservoir pressure), initial oil-gas ratio of the reservoir fluid and relative

permeability as a function of oil saturation. In addition, whether or not it is modelled as a 2D fracture, including the fracture tip effects, or a 1D fracture with only flow perpendicular to the fracture also comes in to play.

4.1 Base Case - Gas Condensate

Initial Reservoir Pressure

A reservoir can either be saturated, $p_R = p_{sat}$ or undersaturated, $p_R > p_{sat}$. The saturation pressure, p_{sat}, can either be a bubblepoint for oil reservoirs or a dewpoint for gas reservoirs. For saturated gas reservoirs, oil will immediately starts condensing out of the gas phase when production starts as the pressure is lowered below the dewpoint. For undersaturated reservoirs on the other hand, the reservoir pressure is initially higher than the dewpoint pressure and oil will only come out of solution when $p < p_d$. It appears that for all saturated gas condensate reservoirs the producing oil-gas ratio (r_p) is very low and can be estimated as approximately equal to the in solution oil-gas ratio at the flowing bottomhole pressure, $r_p \approx (p_{wf}$. This implies that no mobile oil is produced, only oil that is carried in solution in the gas phase. For undersaturated gas reservoirs, with the same in situ conditions as for the saturated reservoir, except the initial reservoir pressure is higher than the dewpoint, the producing oil-gas ratio appear to be slightly higher (fig. 4.1). The pressure gradient is steeper with a higher initial reservoir pressure, and the oil that comes out of solution do this closer to the wellbore in a more confined area which leads to a larger build up of oil saturation. The oil saturation in parts of the reservoir, is then large enough for the oil to be mobilized and this oil is therefore produced along with the in solution oil increasing the total oil-gas ratio.

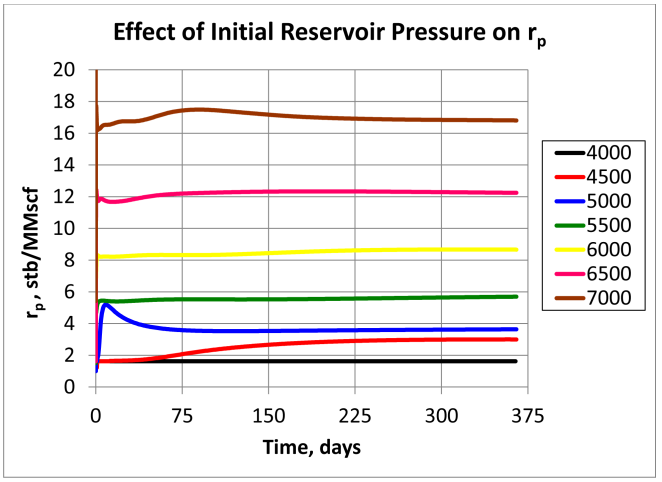

Figure 4.1: *Different producing oil-gas ratios for different initial reservoir pressure.* ($r_{si} = 100$ *stb/MMstb,* $p_d = 3800psia$, $k = 1e-4$ *mD and* $n = 2$*).*

Mobility and Relative Permeability

The mobility, λ, of a fluid, is defined as the ability for the fluid to move. This can be expressed as the ratio of the effective permeability of the fluid to its viscosity. And for a single phase system, it is defined as the ratio of rock permeability to the viscosity of the single phase. For a two phase system on the other hand, the relative permeability also comes into play. For a two phase system, a common variable is the mobility ratio (M) between the different phases, defined as the ratio of the displacing phase to the mobility of the displaced phase Ezekwe [2010]. For shale systems, where water is only present as connate water saturation, it can be considered as a two phase gas-oil system and the mobility ratio is given as:

$$M = \frac{\lambda_g}{\lambda_o} = \frac{k_{rg}\mu_o}{k_{ro}\mu_g} \tag{4.2}$$

Where k_{rg} is the relative permeability of gas, μ_o oil viscosity (cp), k_{ro} the oil relative permeability and μ_g the gas viscosity (cp). The relative permeability directly affects the mobility and mobility ratio of oil and gas. Increasing relative permeability exponents decreases the oil relative permeability at low oil saturation. For gas condensates initial oil saturation is equal to zero, and in practice a increasing relative permeability exponent decreases the relative permeability of oil. Decreasing relative oil permeability increases the mobility ratio, and decreases the producing oil-gas ratio as more gas is produced compared to oil. The different relative permeability curves are shown in figure 4.2 and the

corresponding response of the different relative permeability curves on the producing oil-gas ratio are seen in figure 4.3. It is obvious that relative permeability have an impact on the producing oil-gas ratio in liquid rich gas condensate shale plays. For the two extreme cases, with relative permeability exponents equal to 1 (straight line relative permeability) and relative permeability exponents equal to 3, the producing oil gas ratio is 4 timers higher for n=1 than n=3. Straight line relative permeability is however not really a realistic description of the relative permeability.

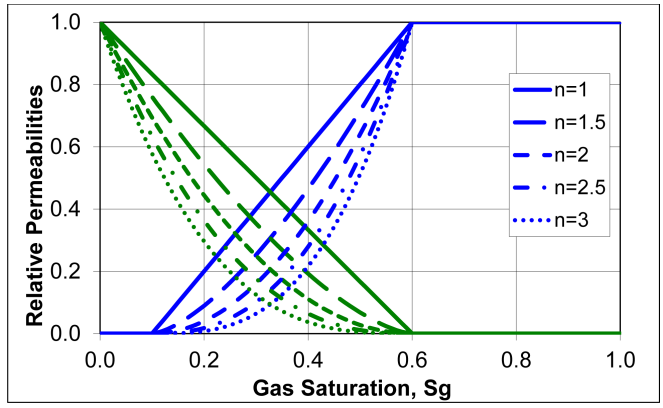

Figure 4.2: *Relative permeability curves for different relative permeability exponents. Oil relative permeability in green and gas relative permeability in blue.*

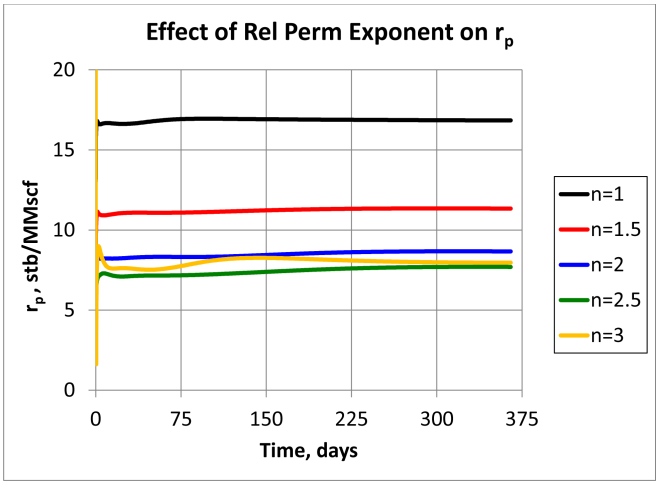

Figure 4.3: *The effect of different relative permeability exponent on the producing oil-gas ratio, r_p. ($r_{si} = 100$ stb/MMstb, $p_d = 3800$ psia, $k = 1e-4$ mD and $p_i = 6000$ psia.)*

Initial GOR

The black oil simulator model is initialized using a initial gas-oil ratio (R_{si}) value. The initial gas-oil ratio of the reservoir fluid determines the richness of the fluid, high gas-oil ratio means a lean gas condensate while a low gas-oil is a richer gas condensate. For gas condensates the value ranges from 3,000 to 150,000 scf/stb. The base case model considered in this thesis have a initial gas-oil ratio of 10,000 scf/stb which corresponds to a initial oil-gas ratio (r_{si}) of 100 stb/MMscf. Particular interesting is the difference (Δr_s) between the initial solution oil-gas ratio (r_{si}) and the solution oil-gas ratio at the flowing bottom hole pressure ($r_s(p_{wf})$). The amount of oil that condenses out in the reservoir can be written as:

$$V_o = \Delta r_s Q_g = (r_{si} - r_s(p_{wf}))Q_g \tag{4.3}$$

Where V_o is oil volume (stb) and Q_g is the cummulative gas production (MMscf). Assuming that all of the oil that comes out of solution stays immobile, the average saturation in the region where the condensing occurs ($p < p_d$) are given as:

$$\bar{S_o} = \frac{(r_{si} - r_s(p_{wf}))Q_g}{5.615 x_f h x \phi 2N} \tag{4.4}$$

Where $\bar{S_o}$ is the average saturation, Q_g is the cumulative gas produced (MMscf),

x is the distance from the fracture to the point where $p = p_d$ (ft), ϕ is the porosity of the rock and N is the number of fractures. For the oil to be mobilized the oil saturation have to be at least higher than the residual oil saturation, in this case equal to 0.2. The initial richness (r_{si}) of the fluid directly influences the oil saturation and will therefore also influence the producing oil-gas ratio. Low r_{si} yields a lower producing oil-gas ratio while a high r_{si} yields a higher producing oil-gas ratio producing at the same bottomhole pressure. Simulation results for different initial oil-gas ratios are plotted in figure 4.4 clearly showing an increasing producing oil-gas ratio with increasing richness of the reservoir fluid. It is also important to notice that from equation 4.4 it follows that the oil saturation build up ($\frac{d\bar{S_o}}{dt}$) is a direct function of the gas rate per pore volume, $\frac{q_g}{x_f h x \phi 2N}$.

$$\frac{d\bar{S_o}}{dt} = \frac{(r_{si} - r_s(p_{wf}))q_g}{5.615 x_f h x \phi 2N} \tag{4.5}$$

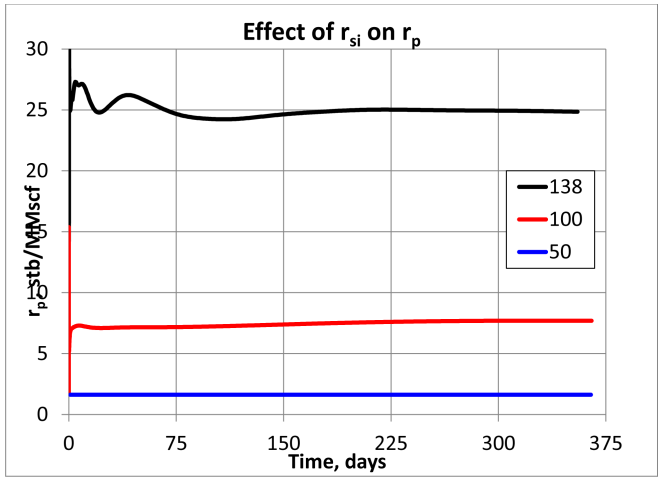

Figure 4.4: *Different producing oil-gas ratios for different initial oil-gas ratios. ($k = 1e-4$ mD, $p_i = 6000$ psia and n=2.)*

Bottomhole Pressure

The total oil rate are given by equation 4.1 and is equal to the sum of the production of free oil and oil that is carried in solution in the gas phase. As the solution oil-gas ratio is strongly dependent on pressure (ref. fig 3.2) the oil rate and hence the producing oil-gas ratio will be a function of the producing bottomhole pressure (fig. 4.5). The producing oil-gas ratio is increasing with

increasing producing bottomhole pressure. Producing at the dew point pressure (3800 psia) and above, the reservoir fluid is single phase gas with a producing oil-gas ratio equal to the solution oil-gas ratio. Producing at lower bottomhole pressures, the pressure drops below the dewpoint pressure and large amount of oil is lost.

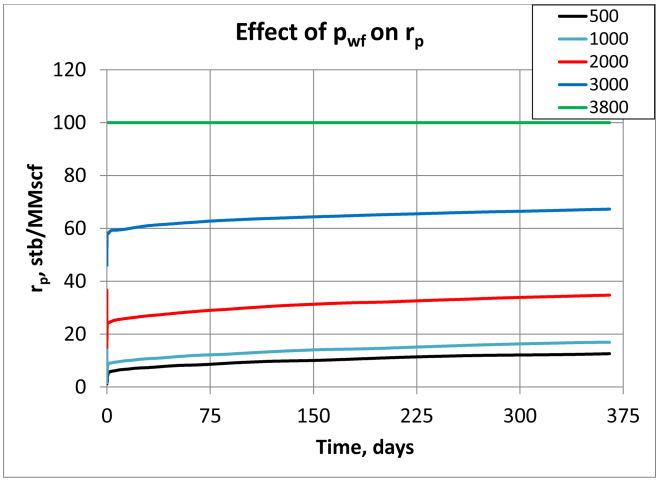

Figure 4.5: *Different producing oil-gas ratios for different producing bottomhole pressure. ($k = 1e-4$ mD, $p_i = 6000$ psia and n=2.)*

2D vs 1D

For 2D models the producing oil-gas ratio are higher than for 1D case (fig. 4.6). The primary factor for this is the fracture tip effects producing more oil. At the fracture tip, the gas flows radial to the fracture (instead of linear). The pore volume close to the fracture tip, where oil starts coming out of solution, is therefore small compared to the amount of pore volumes of gas that passes through. The build up of oil saturation in this near fracture region builds up quicker as the oil saturation is directly linked to the flow rate per pore volume (ref. equation 4.5). This will be discussed more thoroughly in section 5.3

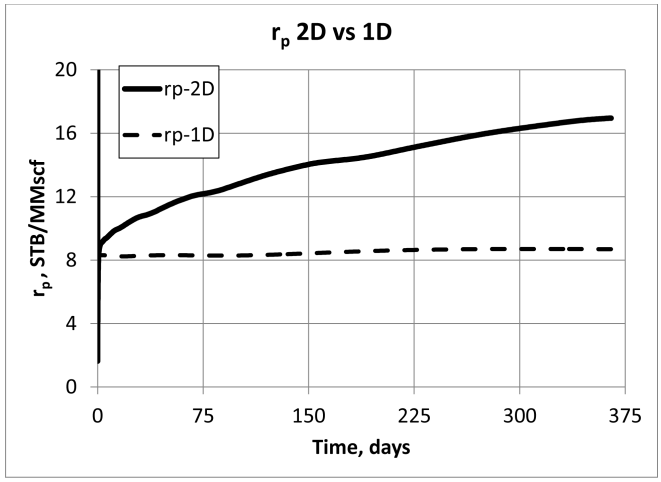

Figure 4.6: *Different producing oil-gas ratios for 1D case (dotted line) and 2D case (solid line).($r_{si} = 100$ stb/MMstb, $p_d = 3800$ psia, $k = 1e-4$ mD, $p_i = 6000$ psia and $n = 2$.)*

4.2 Oil Reservoirs

For liquid rich reservoirs saturated with oil (S_g=0), the producing oil-gas ratios behave differently. The oil will always be mobile in the reservoir and problems with insufficient oil saturation is not encountered. However, as the pressure drops below the bubblepoint pressure (p_b), gas starts coming out of solution. The gas phase mobility is far greater than the oil phase mobility. For gas heavy oil systems (near critical oil) a large amount of gas will come out of solution. The gas will flow more easily towards the fracture because of a higher mobility and "block" some of the oil and reducing the producing oil-gas ratio (fig. 4.7). For richer oil systems (less gas) the amount of gas that comes out of solution are not that significant and will not effect the producing oil-gas ratio in the same way and the producing oil-gas ratio are approximately equal to the initial oil-gas ratio (fig. 4.7).

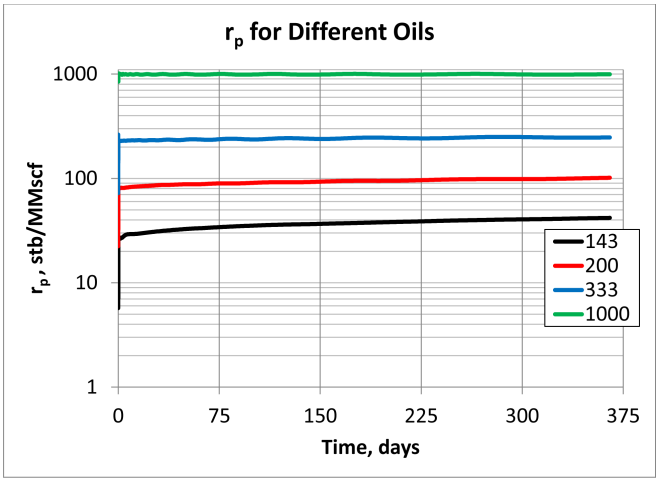

Figure 4.7: *Different producing oil-gas ratios for different initial oil-gas ratios for reservoir saturated with **oil** for 2D reservoir model. ($k = 1e{-}4$ mD, $p_i = 6000$ $psia$ and $n = 2$.) and relative permeability exponents equal to 2.*

Chapter 5

Near Fracture Condensate Build Up

As discussed in section 2.5.1 and chapter 4 liquids will start to come out of solution as soon as the dewpoint pressure is reached and there will be two-phases in the reservoir. The pressure is less than the dewpoint pressure near the well/fracture as the pressure decreases towards the wellbore producing at a low flowing bottomhole pressure (p_{wf}). For gas condensate reservoirs, an oil bank starts building up near the wellbore where $p < p_d$ [Fevang and Whitson, 1995, McCain Jr. and Alexander, 1992]. A gas condensate reservoir can be divided into three regions[Fevang and Whitson, 1995]:

1. **Region 1:** Near wellbore region where the oil saturation is sufficient for the oil to be mobilized. Both oil and gas flow simultaneously.
2. **Region 2:** Intermediate region where condensate is building up. The oil saturation is not high enough for the oil to be mobilized. Primarily gas flow.
3. **Region 3:** Outer reservoir region. Containing only original reservoir gas above dew point pressure.

In region 1 the situation is stable, where everything that goes into region 1 is produced. The composition of the mixture is constant in region 1 and equal to the producing wellstream composition. Hence, the pressure, p*, at the border between region 1 and region 2 is equal to the dewpoint of the produced wellstream. In region 2, the composition is not constant. Heavy components (oil) fall out as

condensate and oil saturation builds up. The pressure at the border of region 2 and 3 equals the dewpoint pressure of the initial reservoir gas. The extent and size of the regions changes as a function of time. All regions may be present at the same time during production, but the extent of the regions may vary from reservoir to reservoir. In some cases region 1 will be very small and in other cases region 2 may be very small. Since a build up of oil saturation reduces the relative permeability of gas, the well deliverability is reduced compared to a well producing only wet or dry gas. This is discussed by Fevang and Whitson [1995] among others and is often known as the condensate blockage effect. The well deliverability including the blockage effect can be calculated in different way. Either as including a blockage skin factor or using the approach of Fevang and Whitson [1995] which is discussed below. The rate equation in black oil terms for a gas condensate may be written as:

$$q_g = C\beta_s \frac{R_{gas}T_{sc}}{p_{sc}} \int_{p_{wf}}^{p_R} \left(\frac{k_{ro}}{B_o\mu_o} R_s + \frac{k_{rg}}{B_g\mu_g} \right) dp \tag{5.1}$$

Where C is a constant containing important reservoir parameters such as permeability (k), reservoir thickness (h), drainage radius (r_e), wellbore radius (r_w) and skin factor (s):

$$C = \frac{kh}{ln(r_e/r_w) - 0.75 + s} \tag{5.2}$$

β_s is a unit conversion factor, R_{gas} is the universal gas constant, T is temperature, p is pressure, k_{ro} and k_{rg} are relative permeability of oil and gas respectively, B is the formation volume factor, μ_o and μ_g is the viscosity of oil and gas respectively. Equation 5.1 differs from the regular gas pseudopressure equation by the inclusion of the oil phase black oil properties and relative permeabilities. The integral in equation 5.1 goes from p_{wf} to p_R and is hard to evaluate. However, by introducing the three different regions the integral can be split into [Fevang and Whitson, 1995]:

$$\int_{p_{wf}}^{p_R} \left(\frac{k_{ro}}{B_o\mu_o} R_s + \frac{k_{rg}}{B_g\mu_g} \right) dp = \int_{p_{wf}}^{p^*} \left(\frac{k_{ro}}{B_o\mu_o} R_s + \frac{k_{rg}}{B_g\mu_g} \right) dp + \int_{p^*}^{p_d} \left(\frac{k_{rg}}{B_g\mu_g} \right) dp + k_{rg} \int_{p_d}^{p_R} \left(\frac{k_{rg}}{B_g\mu_g} \right) dp \tag{5.3}$$

In region 1 both oil and gas are mobile and the integral has to be evaluated for both oil and gas. In region 2, only gas is mobile, but the relative permeability of

gas is dependent on the oil saturation. In region 3, the integral can be evaluated as the normal gas pseudopressure integral with the relative permeability of gas equal to the relative permeability of gas at initial water saturation. Fetkovich et al. [1986] derived an expression for the relative permeability relationship between oil and gas in terms of PVT properties (formation volume factors (B_o and B_g), producing gas-oil ratio (R_p), solution gas-oil ratio (R_s), solution oil-gas ratio (r_s) and viscosities (μ_o and μ_g)) for volatile oil and gas condensates.

$$\frac{k_{rg}}{k_{ro}} = \left(\frac{R_p - R_s}{1 - r_s R_s}\right) \frac{\mu_g B_g}{\mu_o B_o} \tag{5.4}$$

It can also be shown that the relative permeability relationship can be expressed in terms of the oil relative volume during a constant composition expansion test, V_{roCCE}. $V_{roCCE} = \frac{V_o}{V_o + V_g}$ and can therefore replace R_p, R_s, r_s, B_g and B_o and equation 5.4 can be written as:

$$\frac{k_{rg}}{k_{ro}} = \left(\frac{1}{V_{roCCE} - 1}\right) \frac{\mu_g}{\mu_o} \tag{5.5}$$

Equation 5.5 can easily be calculated using a PVT program (PhazeComp) to calculate V_{roCCE} and the viscosities of the producing wellstream at different pressures. The $\frac{k_{rg}}{k_{ro}}$ relationship from PVT properties can be compared to reservoir simulator output to check whether or not region 1 exists.

Fevang and Whitson [1995] shows that equation 5.5 holds for vertical, horizontal and vertical fractured wells. Equation 5.5 can only be used in region 1, where the composition is constant and equal to the wellbore composition. This thesis will also show that it holds for horizontally fractured wells in tight reservoirs as long as the region 1 is stable. However, there also exists a significant transition region between region 1 and 2, where the oil saturation is high enough to flow, but the oil is practically immobile. To be able to mobilize the liquid dropout a significant amount of pore volumes have to pass through. In high kh wells and in radial wells, the majority of the condensate gets mobilized and region 1 is the dominate region. However, in unconventional reservoirs with ultra low permeability, this is not the case. These wells are completed as long horizontal wells, with transverse hydraulically induced fractures as discussed in section 2.3.1. This creates a large crossectional area to flow, and the number of pore volumes passing through is not sufficient to build up a mobile oil region. Region 2 is therefore the dominating region together with region 3. The consequence of this is that the producing oil gas ratio (r_p) is much lower than the initial solution oil-gas ratio (r_{si}) in unconventional liquid-rich gas condensate shale wells as discussed by Whitson and Sunjerga [2012].

5.1 Radial Model

A non-fractured vertical well model in a tight shale gas reservoir was created to compare the results from a conventional to a non-conventional reservoir and from a vertical well (radial model) to a horizontally fractured well. The radial model is based on the same fluid and rock properties as the base case model discussed in section 3.1 for liquid rich shale. The simulator used is SENSOR running compositional simulations with radial grid for 100 days. The $\frac{k_{rg}}{k_{ro}}$ relationship is calculated using equation 5.5 with the producing wellstream composition. V_{roCCE} and viscosities are calculated using the PVT program PhazeComp. The result of these two different approaches for finding $\frac{k_{rg}}{k_{ro}}$ are shown in figure 5.1. There is a very good correlation between the calculated and the simulated results and it can be concluded that region 1 exists to a distance of approximately 1.5 feet from the centre of the wellbore. The producing wellstream has a dewpoint of 3800 psia and a producing GOR of 10,300 scf/stb ($r_p = 97.1$ stb/MMscf). The initial composition have a dewpoint of 3801 psia and a initial solution GOR of 10,254 scf/stb ($r_p = 97.5$ stb/MMscf). This means that the producing wellstream is almost identical to the initial reservoir fluid and $p^* \approx p_d$ meaning that region 2 is almost non-existent and can be neglected. All the initial oil in solution are mobilized and produced as $r_p \approx r_{si}$. The pressure and oil saturation profile plotted versus the distance from the centre of the well is plotted in figure 5.2. It can be concluded that for a vertical well, the producing oil-gas ratio is close to the initial solution oil-gas ratio, even for low permeable reservoirs because of:

1. Logarithmic pressure profile from the well and outwards
2. Sufficient number of pore volumes passes through the near well region to quickly build up a mobile oil saturation

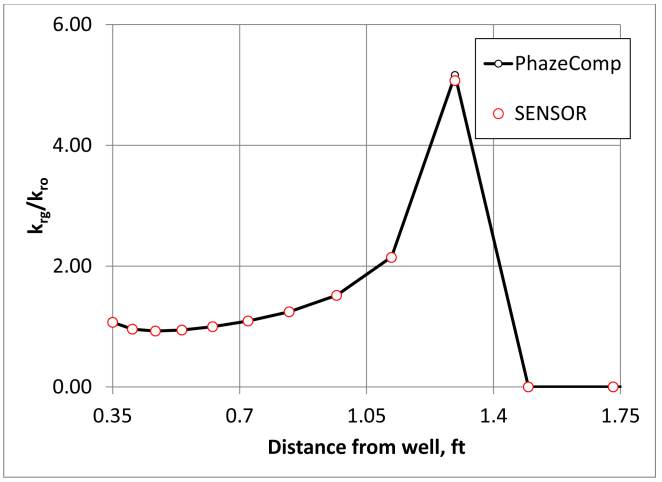

Figure 5.1: *k_{rg}/k_{ro} relationship for both PhazeComp and SENSOR results at 100 days for radial model.*

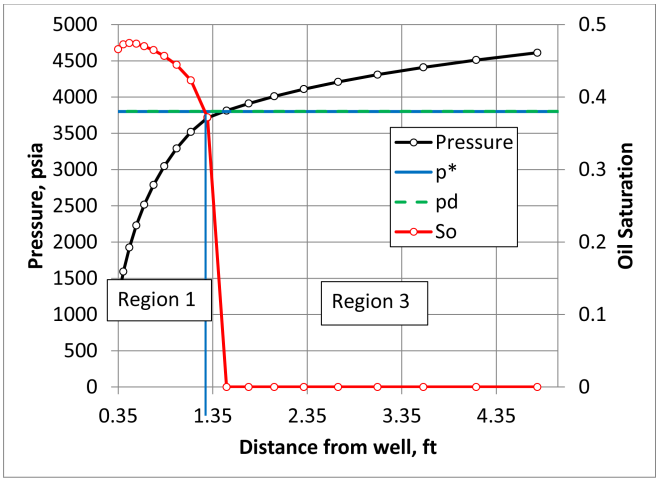

Figure 5.2: *Pressure (black) and saturation (red) profile as a function of distance from the well at 100 days for radial model*

5.2 1D Model

Similar to the radial model, a 1D model for a horizontal well with hydraulically induced fractures was constructed to investigate the existence of the three different regions and their extensions. The model is similar to the base case 1D model discussed in section 3.1 and the approach is similar to the radial model above. The wellstream composition is taken from SENSOR and is used to calculate V_{roCCE}, μ_o and μ_g in PhazeComp to find $\frac{k_{rg}}{k_{ro}}$. For the 1D hydraulically fractured model $r_p \neq r_{si}$ as discussed in section 4. This is clearly different from the radial model where $r_p \approx r_{si}$ and it is expected that in the 1D case, a significant region 2 will also be present. Figure 5.3 displays the $\frac{k_{rg}}{k_{ro}}$ relationship for the 1D model calculated with both SENSOR and PhazeComp after 100 days of production.

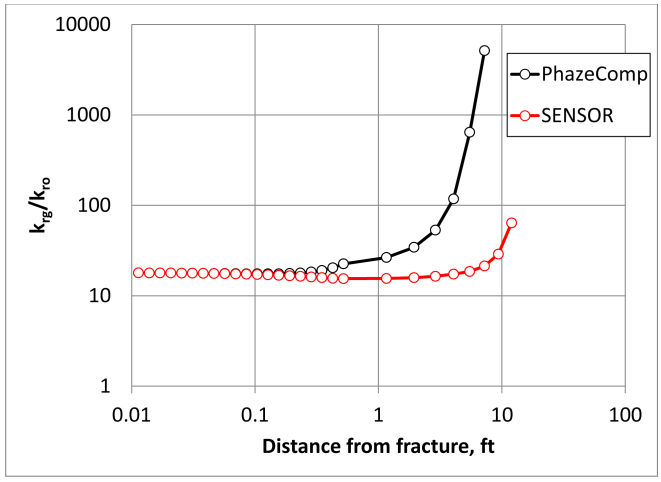

Figure 5.3: *k_{rg}/k_{ro} relationship for both PhazeComp and SENSOR results at 100 days.*

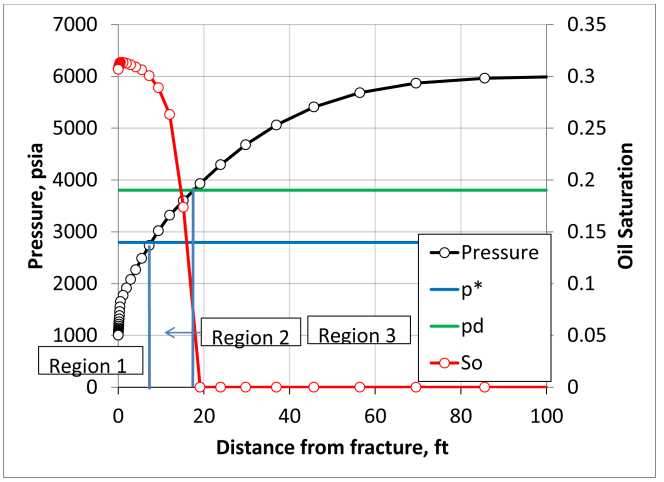

Figure 5.4: *Pressure (black) and saturation (red) profile as a function of the fracture from the well at 100 days. The dewpoint pressure (green) and p* (blue) are plotted to find region 1 and region 2.*

As expected, there also exists a significant region 2 (fig. 5.4), resulting in a lower producing oil-gas ratio. From figure 5.3 it is obvious that the calculations does not match as good as in the radial model discussed above, and it is unclear if the approach is valid. The producing wellstream composition have a dewpoint pressure equal to 2797 psia, which is equal to the pressure at the border between region 1 and 2. At the specific time the flow in the 1D model is still highly transient and infinite-acting and region 1 is not stable (steady state). Because of the infinite acting the primary production from the well comes from areas close to the fracture. Smaller amount of fluids are moved further out as the pressure gradient is smaller. The result of this is that for the sensor calculated values, there exists a transition region between region 1 and region 2 (fig. 5.5). In this transition region the oil saturation is higher than the required saturation for the oil to be mobile, but the oil is in fact practically immobile. Low relative permeability of oil in combination with high viscosity makes the mobility of the oil far less than the mobility of the gas in the transition region. The high mobility ratio in combination with a small pressure gradient makes the oil practically immobile. This causes the discrepancy between the PhazeComp calculated values and the SENSOR calculated values.

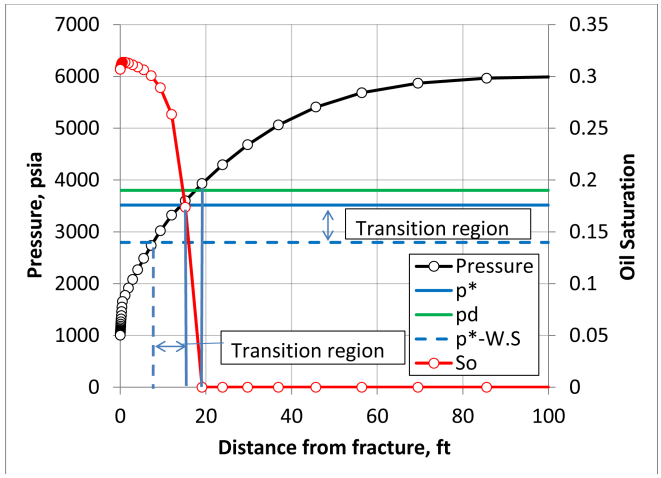

Figure 5.5: *Transition region and discrepancy between SENSOR calculated p^* (blue solid line) and PhazeComp calculated p^*-W.S. (blue dotted line) based on producing wellstream composition.*

After 2500 days, the pressure wave have reached the outer boundary which in this case is the no-flow boundary located between the fractures. The flow is no longer infinite acting and is instead pseudo-steady, where $\frac{dp}{dt} = const.$. This makes region 1 a stable region (steady state). The changes in the extent of region 1 is now smaller and the composition entering region 1 is the same which are produced in the wellbore. The result of the calculations can be seen in figure 5.6. For gas condensates producing with a oil-gas ratio equal to the solution oil-gas ratio at p_{wf} ($r_p = r_s(p_{wf})$) region 1 is very close to the fracture and $p^* \approx p_{wf}$. No free oil is produced, only solution oil.

For the radial model, sufficient numbers of pore volumes flows through the near well region to build up a sufficient oil saturation to mobilize the majority of the oil. For the 1D case, insufficient amount of pore volumes flows through the near fracture region, resulting in a large portion of the oil is lost and a much lower producing oil-gas ratio. The build up of oil saturation is proportional to the rate of gas per pore volume. The rate of gas(q_g) per pore volume ($P.V.$) can be expressed by equation 5.6 for a radial model (with $\theta = 180°$) and equation 5.7 for a 1D model.

$$\frac{q_g}{P.V.} = \frac{2000 q_{radial}}{\pi r^2 h \phi} \tag{5.6}$$

$$\frac{q_g}{P.V.} = \frac{1000 q_{1D}}{2 x_f h x \phi} \tag{5.7}$$

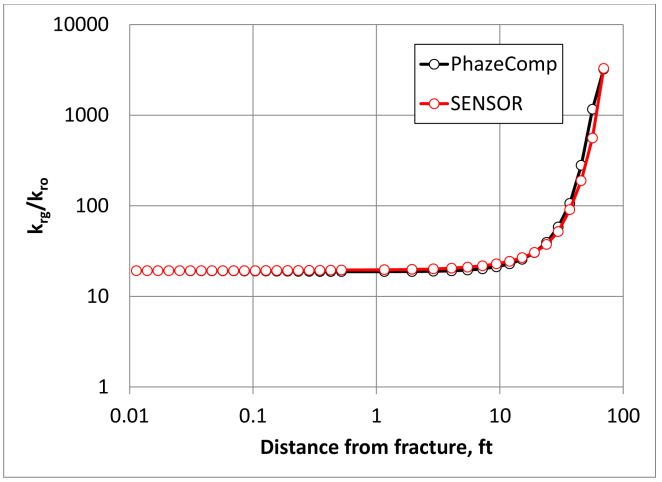

Figure 5.6: *k_{rg}/k_{ro} relationship for both PhazeComp and SENSOR results at 2500 days.*

The distance (r) from the well to the point where the pressure equals the dew-point pressure for the radial model is 1.45 feet while for the distance (x) from the fracture to the point where the pressure equals the dewpoint for the 1D fracture model is 14.27 feet. Rate of gas per pore volume for the radial and 1D cases are calculated in table 5.1. The ratio between the rate of gas per pore volume for radial and 1D fracture model is equal to 58. This is the main reason why the radial model produces with $r_p = r_{si}$ while the 1D fracture model produces with $r_p << r_{si}$.

Table 5.1: Calculated Gas Rate per pore Volume

	$q_g/P.V$
1D	0.84
Radial	48.45
Radial/1D	57.60

5.3 2D Model

For the 2D model the situation is more complex. The flow is not only perpendicular and linear towards the fracture, but the flow is also semi-radial towards the fracture tip. The producing wellstream can then be expressed as a composite of a 1D model and a radial fracture tip model with a drainage angle, θ, equal to 180 degrees:

$$q_{2D} = q_{1D} + q_{radial} \tag{5.8}$$

The cumulative gas and oil production of the 2D model and the composite model consisting of a 1D model and a radial model are shown in figure (5.7) to illustrate that the 2D model is equal to the sum of 1D model and radial model. Even though the contribution from the radial model to the total gas rate is not very large, the contribution from the radial model to the total oil rate is significant. As shown in section 5.1, the oil saturation near the wellbore build up much quicker than for the 1D fracture model as shown in section 5.2 and $p* = p_d$. The producing oil-gas ratio is therefore far greater for the radial model than the 1D fracture model. The producing wellstream for the two dimensional fracture model is therefore a mixture of a very lean fluid produced along the sides the fracture and a richer fluid produced at the fracture tip. Calculating the $\frac{k_{rg}}{k_{ro}}$ relationship using the produced wellstream is therefore not recommended, as it will not be similar to the $\frac{k_{rg}}{k_{ro}}$ relationship outputted from sensor. The produced wellstream composition (z) for the 2D case is equal to:

$$z_{2D} = f z_{1D} + (1 - f) z_{radial} \tag{5.9}$$

Where f is defined as the fraction of molar flow coming from the 1D model.

$$f = \frac{\dot{n}_{1D}}{\dot{n}_{1D} + \dot{n}_{radial}} \tag{5.10}$$

The composition for the 2D model will then not be accurate enough to calculate $\frac{k_{rg}}{k_{ro}}$, neither along the side of the fracture nor outside the fracture tip. The compositions of both the 1D and radial model are more less constant as a function of time (constant producing oil-gas ratios). The 2D composition on the other hand is not constant. The decline of the 1D model is much faster than the radial model (linear versus radial flow), resulting in a changing f and a changing 2D composition as observed by an increasing oil-gas ratio.

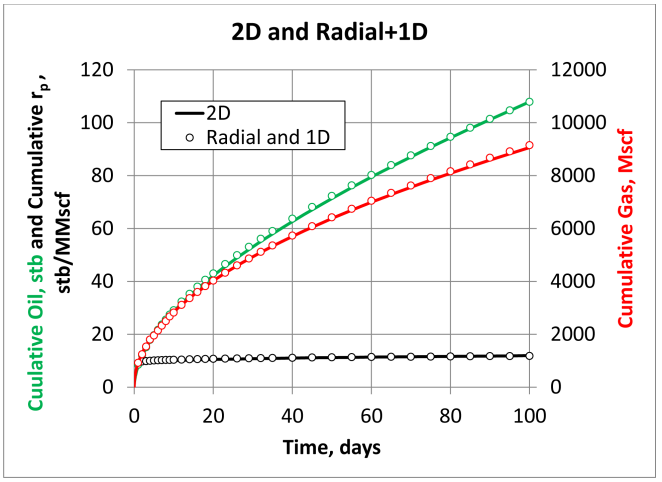

Figure 5.7: *Cumulative oil and gas production as well as cumulative oil-gas ratio for 2D reservoir model (solid lines) and composite of 1D reservoir model and semi-radial model (circles).*

Chapter 6

Optimization of Liquid Rich Shale Gas

As discussed in chapter 4, the producing oil-gas ratio of a liquid-rich shale reservoir is significantly less than both the initial oil-gas ratio and less than what would have been expected from a equivalent conventional reservoir. It is further discussed in chapter 5 where it is concluded that for a shale reservoir with low permeability and hydraulically induced fractures, the flow area is too large to build up a sufficient oil saturation to produce mobile oil in the near fracture area. Instead a large portion of the oil that comes out of solution are left behind in the reservoir. In conventional reservoir one method to counteract this problem would be to inject either water or gas to keep the reservoir pressure higher than the saturation pressure and increase the oil recovery. This is however not thought to be beneficial in unconventional reservoirs as the permeability are way too low to get any benefit without having a very close well spacing. Different approaches are therefore needed in ultra-low permeability reservoirs to increase oil recovery. In the end, the oil recovery has a direct impact on the bottom line of a company. In this chapter, the effect of producing at a higher bottomhole pressure to reduce the amount of oil that comes out of solution, will be studied and discussed. This may increase the oil recovery and the net-present value (NPV) of the asset. Producing at a higher bottomhole pressure (lower drawdown) will reduce the gas rate of the well, but it will also increase the oil-gas ratio as the producing oil-gas ratio is a function of the bottomhole pressure, and in some cases the producing oil-gas ratio is equal to the solution oil-gas ratio at the bottomhole pressure. As discussed in section 2.4, oil is a more valuable commodity than gas. Therefore

an increased bottomhole pressure may actually lead to a higher net present value even though the gas rate is decreased. In this chapter the focus is to optimize oil production and hence optimize the net present value by changing the bottomhole pressure (p_{wf}) as the producing oil-gas ratio is strongly dependent on p_{wf} as seen in figure 4.5. NPV are given by equation 2.8 with a discount rate of 10%, oil price of 100 USD/stb and a gas price of 3 USD/Mscf as the base case. In this thesis only the **revenue** of a project is considered and the net present value is only calculated from the **revenue** generated by the oil and gas production given by the reservoir simulator. The expenses are assumed to be the independent of the producing bottomhole pressure and is therefore neglected in this analysis. The expenses must be included for a complete net present value evaluation of a project, but it does not impact the optimum producing bottomhole pressure. The optimization objective is to find an optimum bottomhole pressure that maximize the net present value and can then be written as:

$$max(NPV) = max\left(\int_0^t \left(\frac{G_p q_g(t) + O_p r_p(p_{wf}) q_g(t)}{(1+d_f)^t}\right) dt\right) \tag{6.1}$$

A dimensional net present value variable, NPV_D is defined as the relationship between the NPV producing at a base case p_{wf}=1000 psia and NPV as a function of p_{wf}. NPV_D is used as a primary optimization variable for the sensitivity studies where it is more important to find out the relative increase rather than the net present value expressed in US dollars.

$$NPV_D = \frac{NPV(p_{wf}) - NPV_{p_{wf}=1000}}{NPV_{p_{wf}=1000}} \tag{6.2}$$

6.1 Base Case - Gas Condensate

The base case are discussed in detail in section 3.1 and the important thing to keep it mind is the low producing oil-gas ratio when producing at a bottomhole pressure equal to 1000 psia. Cumulative producing oil-gas ratio of 13 stb/MMscf compared to a solution oil-gas ratio at dew point pressure of 100 stb/MMscf. There is an obvious upside in terms increased oil recovery. Figure 6.1 shows the calculated net present value for different bottomhole pressures while figure 6.2 displays the cumulative oil and gas production as well as the cumulative oil-gas ratio. The cumulative gas production is steadily decreasing with increasing bottomhole pressure, while the oil production is increasing to a maximum at

3800 psia before it decreases proportional to the decrease in gas production. A significant part of the oil produced, is produced as solution gas. With increasing bottomhole pressure, the solution oil-gas ratio is also increasing causing a higher oil rate even though the gas rate is decreasing. For $p_{wf} \geq p_d$, the producing oil-gas ratio remains constant at 100 stb/MMscf (equal to the solution oil-gas ratio) and the cumulative oil production decreases at the same rate as the gas rate. The optimum bottomhole pressure for the base case gas condensate is equal to the dewpoint pressure. The optimum bottomhole pressure increases the oil recovery from 0.907% to 2.819% while the gas recovery decreases from 7.172% to 2.819% after 1 year of production. The NPV increases with 0.725 million USD and $NPV_D \approx 20$ %.

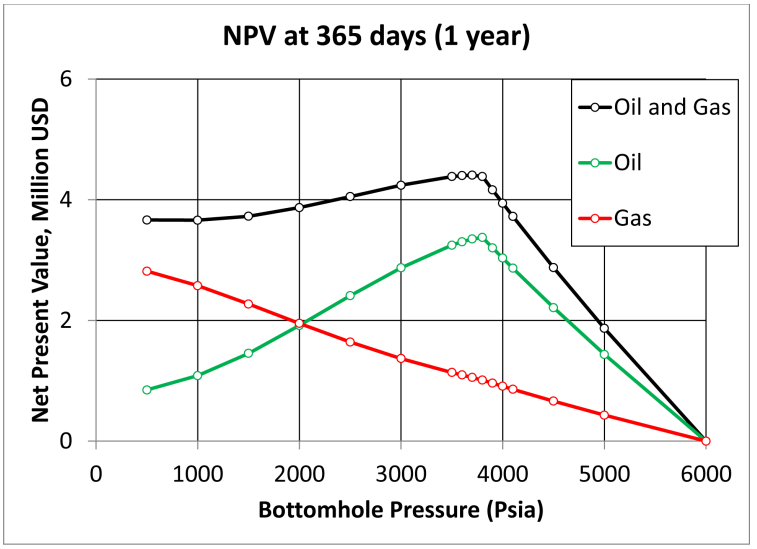

Figure 6.1: *Calculated net present value from the revenues for the base case as a function of bottomhole pressure. Total NPV generated from oil and gas sales (black), NPV generated from oil only (green) and NPV generated from gas only (red). (r_{si} = 100 stb/MMscf, p_d = 3800 psia, p_i = 6000 psia and $k = 1e-4$ mD.)*

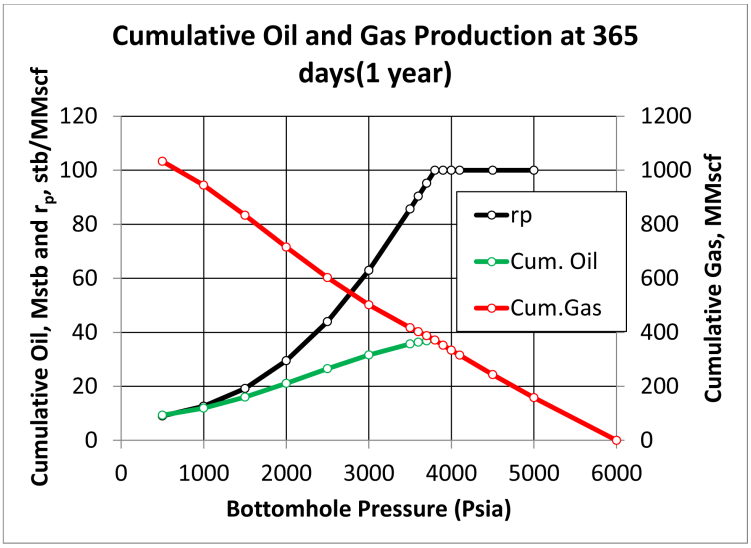

Figure 6.2: *Cumulative oil production (green), gas production (red) and producing oil-gas ratio (black) as a function of bottomhole pressure.* (r_{si} = 100 *stb/MMscf,* $p_d = 3800$ *psia,* $p_i = 6000$ *psia and* $k = 1e-4$ *mD)*

6.2 Sensitivity Studies

6.2.1 Permeability

The reservoir rock permeability is a big uncertainty. It may vary from shale play to shale play and there may also be severe internally differences in the same shale play as discussed in section 2. As the range of uncertainty is large, a number of different cases with different rock permeabilities were run to evaluate what impact the reservoir rock has on the net present value as a function of bottomhole pressure. The different cases are also used to evaluate for what ranges in reservoir rock permeability the method of applying a higher bottomhole pressure to increase the net present value is applicable. Figure 6.3 shows the results of these simulated cases. A clear trend is seen as maximum NPV_D increases with decreasing reservoir rock permeability. For most cases the obvious choice of a optimum bottomhole pressure is close to the dewpoint pressure (3800 psia). It should also be noted that the effect is severely decreasing for reservoir rock permeability equal to 1e-3 mD and 5e-4 mD and for these cases the optimum bottomhole pressure is not equal to the dewpoint pressure. The optimum bot-

tomhole pressures are in between the base case bottomhole pressure of 1000 psia and the dewpoint pressure of 3800 psia, where both an effect of increased oil-gas ratio and high gas rate gives the highest net present value. For any reservoir rock permeability less than 1e-4 mD producing at a higher bottomhole pressure should be considered.

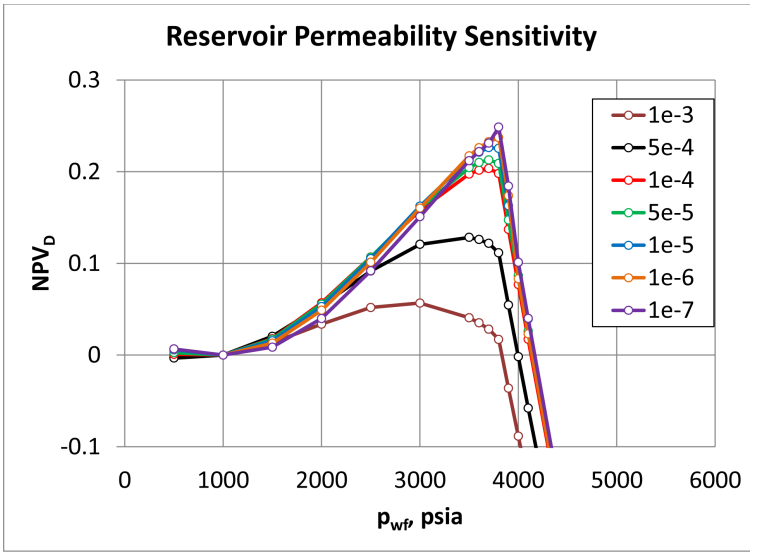

Figure 6.3: *NPV_D as a function of p_{wf} for different reservoir rock permeability ranging from 1e-3 mD to 1e-7 mD after 365 days of production for the base case model ($r_{si} = 100$ stb/MMscf, $p_d = 3800$ psia and $p_i = 6000$ psia).*

6.2.2 Initial Reservoir Pressure

The initial reservoir pressure, p_i, is another important property considering optimizing of net present value of liquid rich shale gas. Not only does it affect the production rates, but also the producing oil-gas ratio. As seen in figure 4.1, the producing oil-gas ratio is varying for different initial reservoir pressure producing at a constant bottomhole pressure equal to 1000 psia and the producing oil-gas ratio is directly impacting the net present value calculations as a function of bottomhole pressure. The figure also shows that for initial reservoir pressure less than 4000 psia (slightly undersaturated and saturated reservoirs) $r_p = r_s(p_{wf}) \approx 1.6$ stb/MMscf even though the initial solution oil-gas ratio, $r_{si} = 100$ stb/MMscf. The difference between the producing oil-gas ratio and initial solution oil-gas ratio is

not the only important factor. A significant pressure difference between the reservoir and the well is also required to get high enough rates. Producing at a bottomhole pressure equal to the dewpoint pressure may not be beneficial for these low pressure reservoirs. Net present value calculations for different initial reservoir pressures are shown in figure 6.4 with a clear increasing NPV_{D} with increasing p_i. For very high initial reservoir pressure ($p_i = 9000psia$), r_p is higher than for lower initial reservoir pressures producing at the same p_{wf}. High initial reservoir pressure increases the gas rate and in terms increases the build up of oil saturation, creating more mobile free oil in the reservoir, resulting in a higher producing oil-gas ratio. The increased r_p results in a smaller Δr_s, and therefore decreases the ratio of oil recovery producing at a bottomhole pressure equal to the dewpoint pressure compared to producing at a low bottomhole pressure. This in turn reduces NPV_{D} for $p_i = 9000psia$ compared to $p_i = 8000$ and $p_i = 6000$ psia.

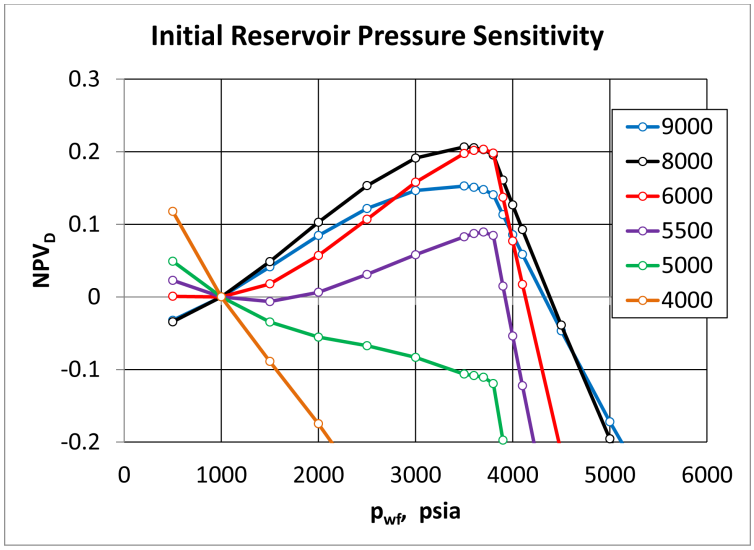

Figure 6.4: *NPV_D as a function of p_{wf} for different initial reservoir pressure ranging from 4000 psia to 9000 psia after 365 days of production for the base case model ($r_{si} = 100$ stb/MMscf, $p_d = 3800$ psia and $k = 1e-4$ mD.*

6.2.3 Initial Oil-Gas Ratio

Is the approach of producing at a bottomohole pressure close to the dewpoint pressure only valid for rich gas condensates or is it universal for most gas condensates? The producing oil-gas ratio which is a particular important parameter for this study and are plotted in figure 4.4 for different gas condensate fluids(different initial oil-gas ratios). A key variable is the difference between the initial oil-gas ratio and producing oil-gas ratio. In table 6.1 a set of different initial oil-gas ratios and corresponding dewpoint pressures are listed which are used in this sensitivity study. All of them are plausible Eagleford liquid rich shale gas condensate fluids. It should be noted that an initial oil-gas ratio of 138 stb/MMscf

Table 6.1: Initial Oil-Gas Ratio and Corresponding Dewpoint Pressure

r_{si} stb/MMscf	p_d psia
138	3909
120	3859
100	3799
80	3661
50	3333

corresponds to a critical fluid, where it is hard to distinguish between the oil and gas phase. Net present value are calculated for the different oil-gas ratios for different bottomhole pressures and plotted as NPV_D versus bottomhole pressure in figure 6.4. For all cases producing at a higher bottomhole pressure approximately equal to the dewpoint pressure is the optimum bottomhole pressure. The optimum bottomhole pressure is also clearly a function of dewpoint pressure as the fluid with r_{si}=50 stb/MMscf the optimum bottomhole pressure is equal to 3300. However, for the critical fluid with r_{si}=138 stb/MMscf the producing bottomhole pressure is **not** the dewpoint pressure, but instead close to 3000 psia, around 1000 psia less than the dewpoint pressure. The critical fluid is the richest fluid, and more oil have potential of coming out of solution as the difference between initial solution oil-gas ratio and solution oil-gas ratio at the bottomhole pressure, Δr_s=136 stb/MMscf. This means that the oil saturation builds up quicker and producing at around 3000 psia the producing oil-gas ratio is equal to the initial oil-gas ratio. It can anyway be concluded that the approach of producing at a higher bottomhole pressure is valid for a range of different initial oil-gas ratios.

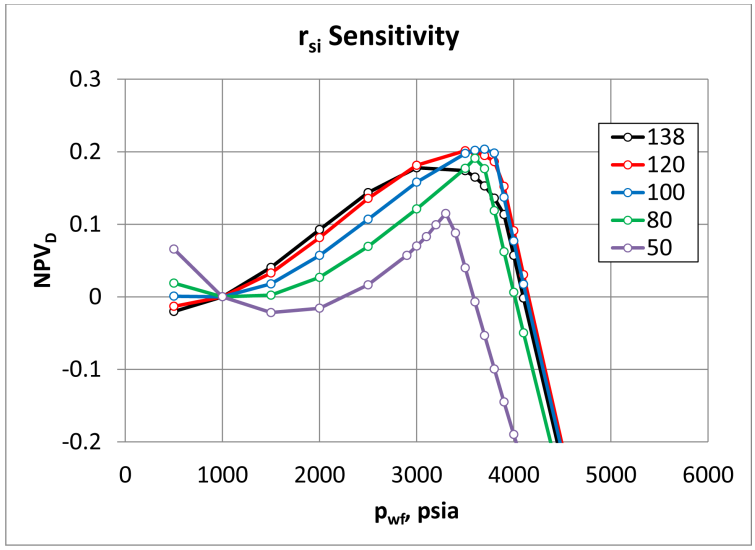

Figure 6.5: *NPV_D as a function of p_{wf} for different initial oil gas ratios ranging from 50 stb/MMscf to 138 stb/MMscf after 365 days of production for the base case model ($p_i = 6000$ psia and $k = 1e-4$ mD).*

6.2.4 Economics

As discussed in section 2.4 the oil and gas prices varies. The historical data of oil and gas prices are shown in figure 2.4 and large fluctuations in oil and gas prices are observed. These fluctuations are often associated with political events or general economical trends. General economic expansion in key markets will cause the oil price to grow and economic recessions will cause the oil price to fall. This is best illustrated in the 2000s where a booming economy, both in the US and worldwide, caused a high demand for oil while the supply of oil did not catch up. The oil price grew to a staggering value close to 150 US dollar per barrel. When the financial crisis struck, the oil price plummeted to around 40 US dollar per barrel. Another important factor to keep in mind when considering the oil and gas prices, are that oil is normally considered a global commodity while gas is normally considered a local commodity. This means that the oil price is more or less the same all over the world while the gas price varies from market to market. Gas requires a certain distribution network and is often transported in pipelines from areas where production is high to areas where the demand is high. Gas is more difficult to transport from market to market and if either the production goes up or the demand goes down in the same market, the gas price will change,

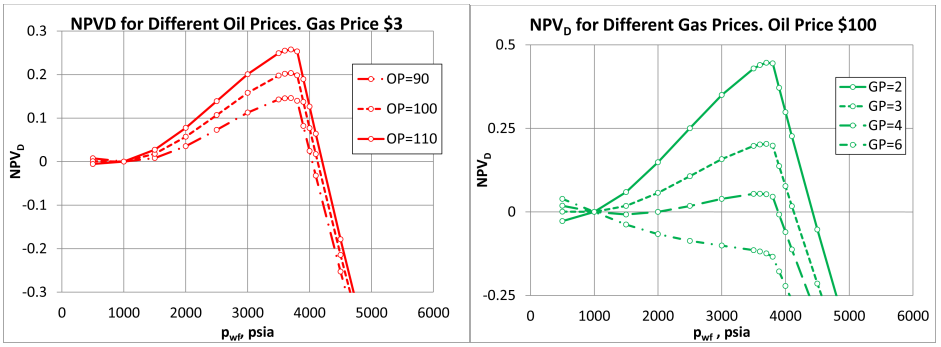

(a) Oil price (OP) sensitivity. Gas price constant at 3 USD/MMscf

(b) Gas price (GP) sensitivity. Oil price constant at 100 USD/stb

Figure 6.6: *Oil and gas price sensitivity for base case reservoir model for 365 production days.* (r_{si} = 100 *stb/MMscf,* p_d = 3800*psia,* p_i = 6000*psia and* $k = 1e-4$ *mD)*

but only in that market. Gas can be transported as LNG, but the LNG facilities at the moment are not sufficient to equal out the differences in gas price from market to market. Predicting the future oil and gas prices are therefore extremely difficult, but a sensitivity study with different oil and gas prices were done in this study to see the impact of oil and gas price on the optimum producing bottomhole pressure. The result of this study are seen in figure 6.6 with oil prices ranging from 90 US dollar to 110 US dollar per stock tank barrel and gas prices ranging from 2 US dollar to 6 US dollar per Mscf. It is obvious that the optimum bottomhole pressure is very sensitive to oil and gas prices, and gas price especially. A gas price of 4 USD /Mscf and a oil price of 100 USD/stb is close to a breakeven case, while a gas price of 6 USD/Mscf and a oil price of 100 USD/stb strongly favours production at the lowest possible bottomhole pressure. On the other hand, a gas price of only 2 USD/Mscf increases NPV_D to about 0.4 when producing at a bottomhole pressure equal to the dewpoint pressure.

6.3 Varying Bottomhole Pressure

Section 6.1 shows that the optimum initial producing bottomhole pressure are equal to the dew point of the reservoir fluid (p_{wf}=3800) and not the lowest possible bottomhole pressure. However, producing at a bottomhole pressure equal to

3800 psia there will be a significant potential left in the reservoir at abandonment (when $p_R = 3800psia$). Looking at NPV_D, producing at p_{wf}=3800 for different end production times (fig. 6.7), the increase in net present value is decreasing with end production time indicating that the effect of a higher bottomhole pressure is greatest in the earliest stage of production.

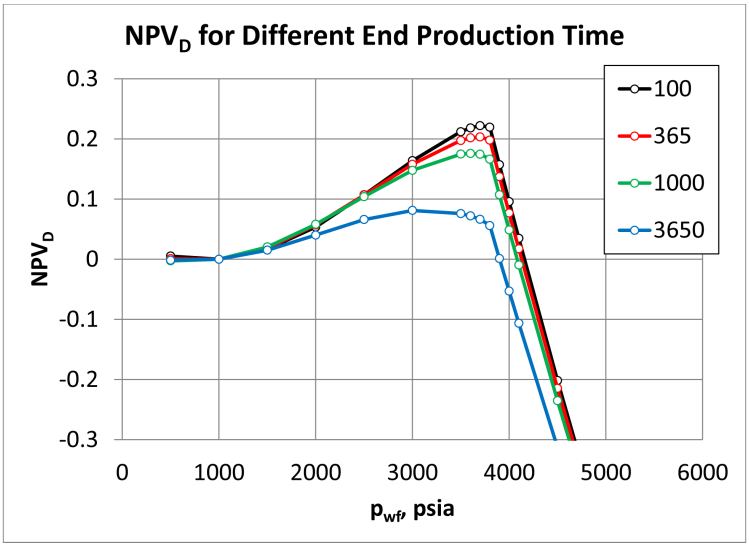

Figure 6.7: *NPV_D as a function of p_{wf} for different end production times (r_{si} = 100 stb/MMscf, p_d = 3800 psia, p_i = 6000 psia and $k = 1e-4$ mD).*

To look at this more closely, two different cases were considered, either producing at a pressure equal to the dewpoint pressure (3800 psia) or producing at a lowest possible bottomhole pressure (500 psia). The producing gas rate will be significantly lower for p_{wf}=3800 psia than p_{wf}=500 psia. Even though the producing oil rate will be higher, at a given point in time the revenue generated from producing at a low bottomhole pressure will exceed the revenues generated by producing at a higher bottomhole pressure. Still, it is important to notice that even after 10 years of production, producing at a high bottomhole pressure still generates a higher net present value than producing at a low bottomhole pressure. At around 4 years of production the rate of revenues generated from producing at p_{wf}=500 psia are equal or grater than producing at p_{wf}=3800 psia (fig. 6.8). This indicates that it would be beneficial to change from a high to a low bottomhole pressure to maximize the net present value of the well. A further 2 cases were considered. One case where changing the bottomhole pressure from

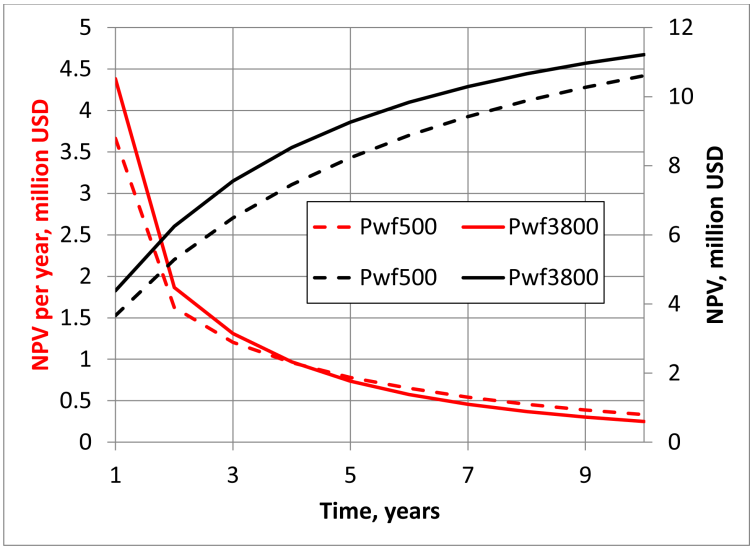

Figure 6.8: *NPV (black) and rate of NPV per year (red) for* $p_wf = 500$ *psia (dotted lines) and* $p_wf = 3800$ *psia (solid lines).* ($r_{si} = 100$ *stb/MMscf,* $p_d = 3800$ *psia,* $p_i = 6000$ *psia and* $k = 1e-4$ *mD*).

3800 to 500 psia after any given time, which was chosen as 2 years in this case. Another case was run to see the effect of producing at a low bottomhole pressure and subsequently changing to a high bottomhole pressure. This case was included to investigate the potential of applying a high bottomhole pressure to wells that have already produced at a low bottomhole pressure. The 4 different cases can then be listed as:

1. **Case 1**: p_{wf} equal to a constant value of 3800 psia for 10 years.
2. **Case 2**: p_{wf} equal to a constant value of 500 psia for 10 years.
3. **Case 3**: p_{wf} equal to 3800 psia for the first 2 years before changing to 500 psia for the last 8 years.
4. **Case 4**: p_{wf} equal to 500 psia for the first 2 years before changing to 3800 psia for the last 8 years.

The effect of changing the bottomhole pressure from high to low yields a significant increase in NPV! One of the important observations is that the gas production rapidly increases after lowering the bottomhole pressure. When producing more oil in the first period of production, less oil will come out of solution and

Table 6.2: Simulation Results for Varying Bottomhole Pressure

Case	RF_o	RF_g	NPV mill. USD	NPV_D
1	9.0%	9.0%	11.21	0.056
2	3.7%	26.3%	10.60	-0.002
3	5.6%	26.5%	12.80	0.205
4	1.6%	11.5%	5.57	-0.476

block (reduce the relative permeability) the gas production in the second period of production. The gas production then quickly catches up with the gas production In fact, the cumulative gas production after only a few years of production equals (and slightly exceeds) the cumulative gas production of case 2, producing at a constant low bottomhole pressure (fig. 6.9). The cumulative oil production increases for the first two years and this increase remains when changing to a lower bottomhole pressure when the production profile follow the production profile of case 2. This gives a recovery of oil and gas after 10 years of production of 5.6% and 26.6% respectively and the calculated NPV_D=0.205 (table 6.2). For the fourth case the situation is completely different and is clearly not favourable. After two years of production at a low bottomhole pressure, the well need a substantial long time (5 years), to build up pressure before even being able to produce anything at p_{wf}=3800 psia!. And even though the producing oil-gas ratio increases after the shut in, the recovery factor of oil and gas are only 1.6% and 11.5% respectively giving a NPV_D=-0.476 (table 6.2). It is therefore **not recommended** to raise the bottomhole pressure up to dewpoint pressure for shale gas wells that have produced for a significant time at a low bottomhole pressure! This method can **only** be used for new shale gas wells or shale gas wells that have produced at a high bottomhole pressure for other reasons. The recovery factor of gas for case 2 and 3 is roughly equal to 26 % while the gas recovery of case 1 is only 9%. The recovery factor for oil is for case 1 9%, case 2 3.7 % and case 3 5.6% (table 6.2). The total net present value versus time for the 4 different cases (fig. 6.10) shows a dramatic increase in the net present value when switching from 3800 psia to 500 psia.

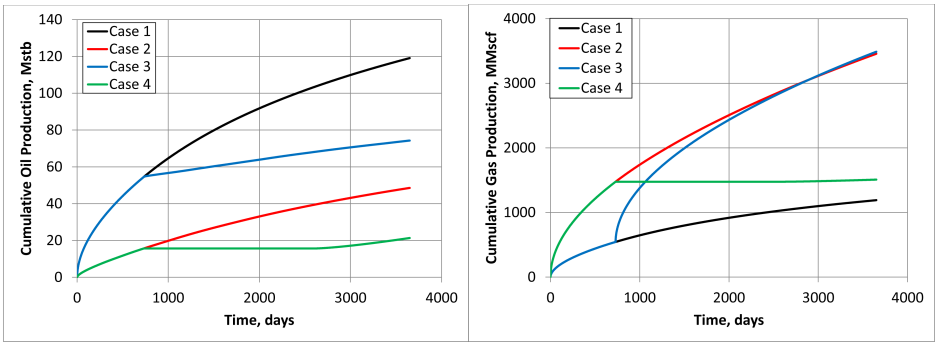

(a) Cumulative Oil Production **(b)** Cumulative Gas Production

Figure 6.9: *Cumulative oil (Q_o) and gas production (Q_g) as a function of time for the 4 different cases. Q_o plotted in the left figure and Q_g plotted in the right figure. ($r_{si} = 100$ stb/MMscf, $p_d = 3800$ psia, $p_i = 6000$ psia and $k = 1e-4$ mD)*

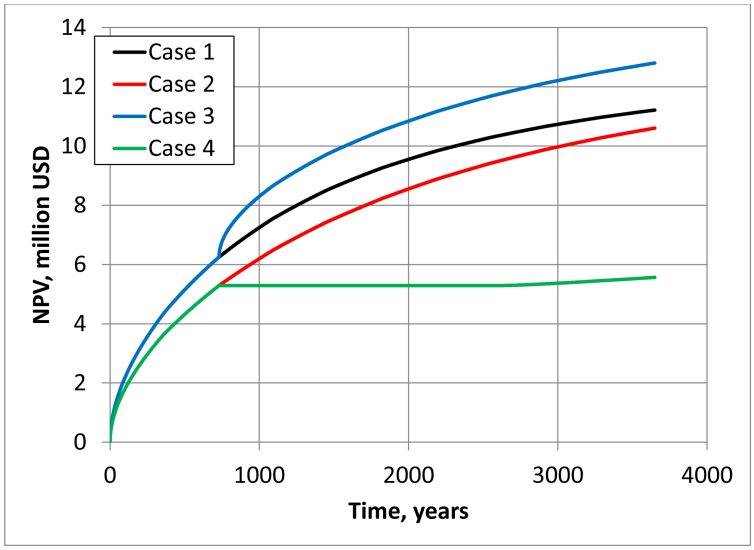

Figure 6.10: *Net present value calculated cumulative revenues for the 4 different cases. ($r_{si} = 100$ stb/MMscf, $p_d = 3800$ psia, $p_i = 6000$ psia and $k = 1e-4$ mD).*

6.3.1 Optimizing Bottomhole Pressure

In case 3, the time when changing the bottomhole pressure from 3800 to 500 psia was chosen arbitrarily. Finding the point in time to change from a higher to a lower bottomhole pressure can be organized as an optimization problem, where the goal is to maximize the net present value. The net present value is a function of the production at p_{wf}=3800 psia and p_{wf}=500 psia. The variable τ denotes the time for changing from p_{wf}=3800 psia to p_{wf}=500 psia.

$$NPV = \int_0^{\tau} CF|_{p_{wf}=3800} dt + \int_{\tau}^{t_p} CF|_{p_{wf}=500} dt \tag{6.3}$$

$\tau = 0$ days is equal to a constant p_{wf}=500 psia and $\tau = 3650$ days is equal to a constant p_{wf}=3800 psia for 10 years. Let q_{g1} and r_{p1} be the gas rate and producing oil-gas rate at p_{wf}=3800 and let q_{g2} and r_{p2} be the gas rate and producing oil-gas rate at p_{wf}=500. The optimization problem can then be defined as:

$$max \left(\int_0^{\tau} \left(\frac{G_p q_{g1}(t) + 10^{-3} O_p r_p q_{g1}(t)}{(1+d_f)^t} \right) dt + \int_{\tau}^{t_p} \left(\frac{G_p q_{g2} + 10^{-3} O_p r_{p2} q_{g2}}{(1+d_f)^t} \right) dt \right) \tag{6.4}$$

Where G_p is the gas price, O_p the oil price and d_f the discount rate. For p_{wf}=3800 r_p=$r_{si}s$=100stb/MMscf=0.1stb/Mscf. For p_{wf}=500 on the other hand, r_p is a function of time. Equation 6.4 can then be reduce to:

$$max \left(\int_0^{\tau} \left(\frac{q_{g1}(t)(G_p + 0.1 O_p)}{(1+d_f)^t} \right) dt + \int_{\tau}^{t_p} \left(\frac{q_{g2}(t)(G_p + O_p r_p(t)}{(1+d_f)^t} \right) dt \right) \tag{6.5}$$

The objective is then to find the time, τ, to change p_{wf} from 3800 to 500 psia that maximizes net present value of the well. To find the right time to change the bottomhole pressure is essential. Changing the bottomhole pressure results in lower producing oil-gas ratios than what could have been achieved. Changing too late will results in a period of production at very low rates. The total NPV is strongly dependent of this τ (fig. 6.11). Producing at a bottomhole pressure of 3800 psia and changing the bottomhole pressure down to 500 psia at the optimum time, the net present value of the revenues generated by the well increases by 24% or 2.56 million US dollar (fig. 6.11). The optimal duration of the first flow period, high bottomhole pressure, is between 1000-2000 days, with 1600 days being the absolute optimal duration. Lowering the bottomhole pressure from 3800 to 500 psia stepwise with intermediate bottomhole pressures over a longer time period

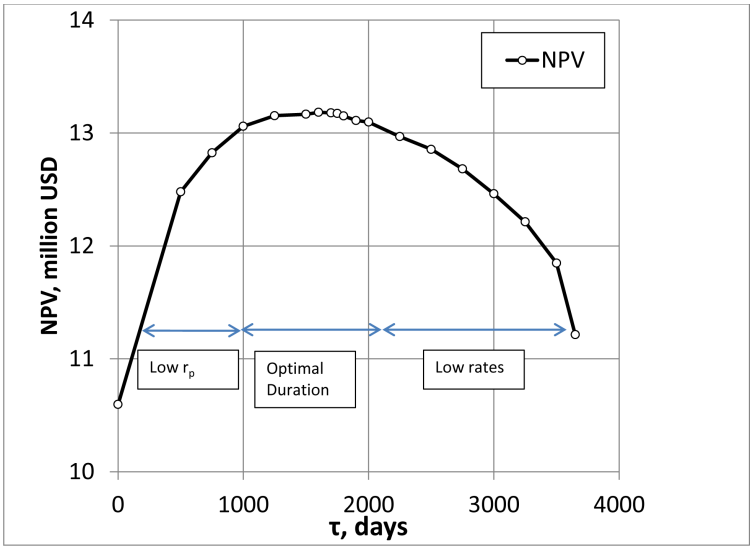

Figure 6.11: *Net present value as a function of the duration of the first flow period ($p_{wf} = 3800psia$) before changing to the second flow period ($p_{wf} = 500psia$). ($r_{si} = 100$ stb/MMscf, $p_d = 3800$ psia, $p_i = 6000$ psia and $k = 1e-4$ mD).*

were also considered. This did not give any conclusive results whether or not it was better or worse to reduce the bottomhole pressure stepwise. The end results in terms of increased net present value was about the same. This approach may on the other hand be easier to implement in practice, as a instantaneously change in bottomhole pressure from 3800 to 500 psia is unlikely.

6.3.2 Liquid Loading

Producing at high bottomhole pressure may cause issues concerning liquid loading. Liquids (oil) starts accumulate in the wellbore because the gas velocity (rate) is not high enough to lift the liquids. There is mainly two reasons why problems with liquid loading arises:

1. High p_{wf} produces low gas flow rates because of reduced pressure drop from the reservoir to the well.
2. To obtain a high p_{wf}, the choke settings must be set such that the tubinghead pressure is also high. There will therefore be a high pressure in the entire tubing. Gas is compressible so to get high enough rates in the

tubing, the surface rates must be even higher.

Turner et al. [1969] proposed an equation for the minimum gas rate (critical gas rate) to lift liquids for gas wells:

$$q_{min} = \frac{172.8\pi r_w^2}{B_g} \frac{(\sigma\Delta\rho)^2}{\sqrt{\rho_g}} \tag{6.6}$$

Where q_{min} is the minimum gas rate to lift (Mscf/d), r_w is the well radius (ft), B_g is the formation volume factor for gas (ft^3/scf), σ is the interfacial tension (dynes/cm), $\Delta\rho$ is difference in density between oil and gas (lb_m/ft^3) and ρ_g is the gas density (lb_m/ft^3) .

Equation 6.6 should be evaluated at the tubinghead where q_{min} is highest. The tubinghead pressure were calculated using the average temperature, average Z-factor equation by Fetkovich [1975]:

$$p_t^2 = \sqrt{\frac{p_{wf}^2}{e^S} + \left(\frac{0.10797D^{-}2.612\bar{T}\bar{Z}}{31.62}\right)^2 \frac{(e^S - 1)}{e^S}} \tag{6.7}$$

Where S is is a hydrostatic term given by:

$$S = 0.0375\frac{\gamma_g TVD}{\bar{T}\bar{Z}} \tag{6.8}$$

For all rates the tubinghead pressure were approximately constant around 2930 psia indicating the hydrostatic pressure drop dominating. For a 5 inch tubing the minimum gas rate to lift liquids is equal to 1888 Mscf/d. Producing at a bottomhole pressure of 3800 psia the well produce less than the minimum gas rate after 25 days of production. One option to counteract liquid loading problems is to use smaller tubing sizes. Smaller tubing size increases gas velocity and therefore the ability to lift liquids. As seen in figure 6.12 using a tubing size of 2 3/8 inches or smaller counteract the problems with liquid loading. The minimum rate to lift is a strongly dependent on the tubinhead pressure (fig 6.13) and changing the tubinghead pressure (and consequently p_{wf}) may be an option to avoid any problems with liquid loading. This will reduce the recovery of oil, but on the other hand any costs associated with artificial lifting are neglected. A final option would be to install artificial lift systems to lift the liquids from the well. This could for example be pumps or gas lift systems.

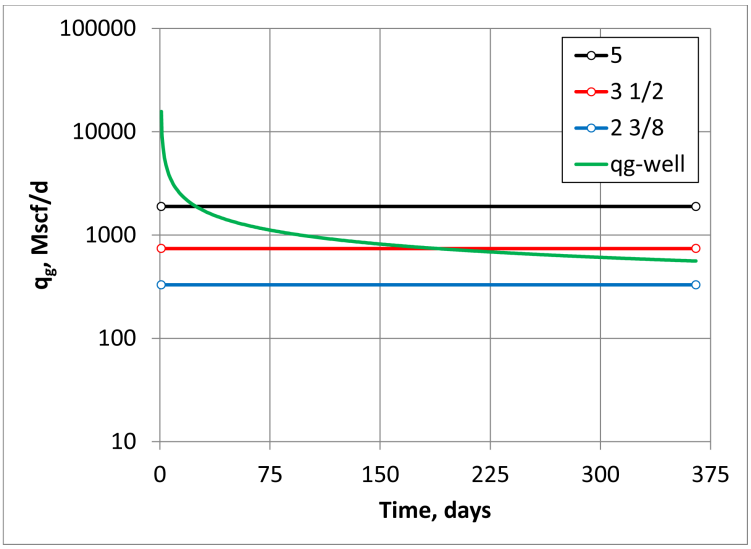

Figure 6.12: *Base case gas condensate p_{wf}=3800 psi gas rate (green) and minimum rate to lift for different tubing sizes.*

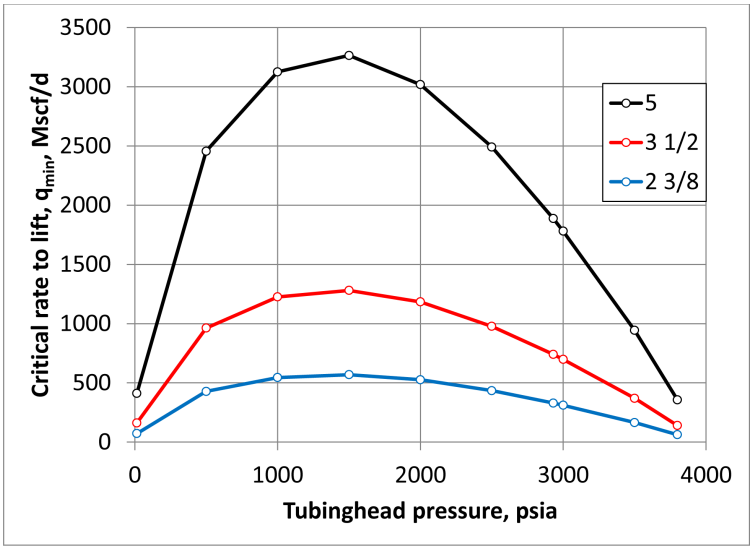

Figure 6.13: *Minimum rate to lift as a function of tubinghead pressure for different tubing sizes.*

6.4 Base Case - Volatile Oil

Until now only reservoirs initially saturated with gas are considered. The fluid in liquid rich shale gas reservoirs can either be in gas or oil phase. For oil phase, the producing oil-gas ratio does not deviate from initial oil-gas ratio nearly as much as for reservoirs with gas phase initially (see section 4.2). However, there is still a significant difference in producing oil-gas ratio for near critical volatile oil systems (fig 4.7) caused by mobility differences between the oil and gas phase when free gas starts coming out of solution. The free gas phase will dominate the flow towards the well and reduce the oil rate. The effect of different bottomhole pressures on the net present value for shale oil reservoirs are also studied with a similar approach as the gas condensate reservoirs. A variety of oils, from volatile oil to near-critical oil are studied (table 6.3). Except initialization with oil instead of gas and different oil-gas ratios, the simulation model is the same as the base case simulation model used in previous chapters ($p_i = 6000$ psia and $k = 1e-4$ mD). For near critical oil systems ($r_{si} = 143$ and $r_{si} = 200$) there is a small effect of producing at a higher bottomhole pressure (fig. 6.14). These system are very gas heavy initially and a lot of gas comes out of solution and "blocks" the oil from flowing freely towards the fractures. However, the optimum bottomhole pressure is not the saturation pressure, but a pressure in between that gives both an increased producing oil-gas ratio and still maintains a high drawdown for higher flow rates. For richer volatile oil systems ($r_{si} = 333$ and $r_{si} = 1000$) the effect of producing single phase oil on increased oil recovery is very small, because less gas comes out of solution that blocks the oil flowing towards the fractures. For richer oil systems the optimum bottomhole pressure is the lowest possible bottomhole pressure (largest drawdown).

Table 6.3: Initial Oil-Gas Ratio for Oil

r_{si} stb/MMscf	R_{si} scf/stb	p_b psia
143	7000	3895
200	5000	3712
333	3000	3152
1000	1000	1453

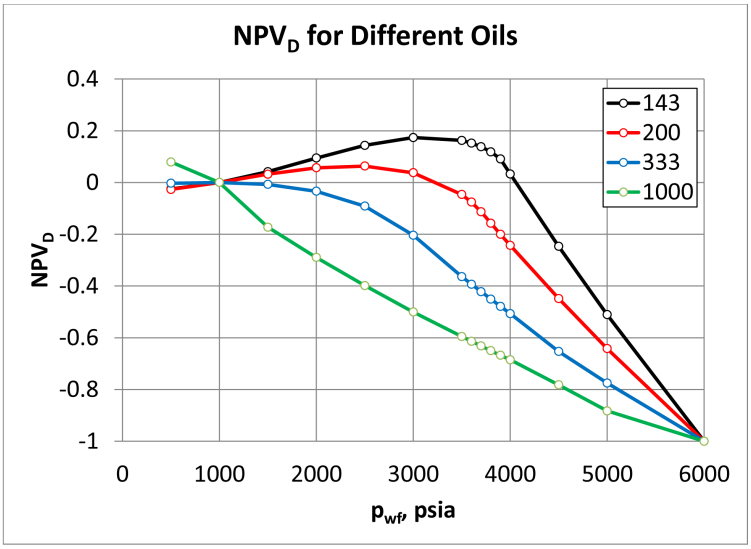

Figure 6.14: *Dimensionless net present value for shale oil with different initial r_{si} ranging from 143 stb/MMscf to 1000 stb/MMscf. (p_i = 6000 psia and k = 1e − 4 mD))*

Chapter 7

Conclusion

This thesis shows interesting and promising results regarding increased oil recovery and increased net present value of liquid rich shale gas wells. To sum up the findings of this thesis the following conclusions can be made:

1. The producing oil-gas ratio for gas condensates is significantly lower than the initial in solution oil-gas ratio ($r_p << r_{si}$). r_p for the base case simulation is approximately 13 stb/MMscf versus r_{si} equal to 100 stb/MMscf.

2. Producing oil gas ratio is dependent on many different parameters. For all saturated cases $r_p \approx r_s(p_{wf})$. For undersaturated cases r_p depends also on initial reservoir pressure, relative permeability and initial oil-gas ratio.

3. For shale reservoirs saturated with oil, the difference between producing and initial solution oil-gas ratio is not as significant. For near critical oils the producing oil-gas ratio differs from the initial solution oil-gas ratio, while for volatile and black oils, the producing oil-gas ratio equals with, good accuracy, the initial oil-gas ratio ($r_p = r_{si}$).

4. For cases where $r_p = r_s(p_{wf})$ region 1, the mobile oil region, is practically non-existent. The produced wellstream composition is equal to the gas composition at p_{wf}. For cases where r_p is slightly higher than $r_s(p_{wf})$, region 1 extends a short distance away from the fracture, but a significant region 2, build up of oil saturation, exists resulting in $r_p << r_{si}$.

5. For infinite acting linear flow a transition region between region 1 and 2 exist. In this region, the oil saturation is above the saturation required to get mobile oil. The mobility of the oil in this region is on the other hand very

small. Low mobility and a low pressure gradient in this region makes the oil practically immobile (and therefore practically a part of region 2). This results in a mismatch between the analytically calculated k_{rg}/k_{ro} and the simulator calculated values for infinite acting linear flow. When pseduo-steady state is reached, the analytically calculated values and simulator values matches with good accuracy.

6. Producing at a higher bottomhole pressure, increases oil recovery as the producing oil-gas ratio increases. Producing at $p_{wf} = p_d$ for the base case gas condensate, increases oil recovery from 0.907 % to 2.819 % after 1 year of production. After 10 years of production, the oil recovery increases from 4.359% to 9.04%. The increased oil production occurs at the expense of reduced gas production, reducing the gas recovery from 7.172% to 2.819% after 1 year of production and from 24.07% to 9.04% after 10 years of production.

7. The increased oil recovery also increases the net-present value of the revenues of the project. Producing at $p_{wf} = p_d$ for 1 year increases the net present value by 0.725 million USD (relative increase, NPV_D=0.198). After 10 years of production the net present value are increased by 0.591 million USD and NPV_D=0.056.

8. The approach of producing at higher bottomhole pressure to be economical requires certain criteria to be met. The reservoir must be have a certain degree of undersaturation, low matrix permeability and a sufficient difference between the producing oil-gas ratio for low bottomhole pressures and the initial solution oil-gas ratio. The relative increase in net present value (NPV_D) increases with increasing initial reservoir pressure (to a certain limit), decreasing permeability and increasing richness of the reservoir fluid.

9. Producing at bottomhole pressure equal to the dewpoint pressure, does not permanently reduce the gas recovery, but the gas production is delayed. When lowering the bottomhole pressure after a period of production at high bottomhole pressure, the gas recovery increases and catches up with the production at a constant low bottomhole pressure quickly. For the base case gas condensate the optimum time to change from high to low pressure is 1600 days which increases the net present value after 10 years of production with 2.56 million USD (NPV_D=0.24).

10. Applying $p_{wf} = p_d$ for wells that have been producing at a low bottomhole pressure for a significant period of time is not recommended. The well require a very long shut in time (years) to recharge back to a reservoir pressure where the well can actually produce.

11. Producing at a bottomhole pressure close to the saturation pressure may also be applied to near-critical and volatile oil systems to increase oil recovery and consequently the net present value. For richer oil systems, the method does not increase the oil or net present value of the well.

Chapter 8

Limitations and Future Work

It is recommended that the option of producing at a higher bottomhole pressure to increase oil recovery and consequently the net present value of shale wells are further investigated. Even though this thesis shows it is definitely a viable options for a range of cases, it also shows that it may be sensitive to a variety of factors. This thesis are limited to simple modelling of reservoirs by conventional reservoir simulators and no history matching, field tests or laboratory tests are performed. This thesis have only looked at planar fractures and different fracture geometry, such as complex fracture network, should be studied if the same effects are present for different fracture geometries. Real field data PVT samples of liquid-rich shale wells should be collected to get a more accurate fluid representation in the simulation model. The fracturing operation and the clean up process of a well have not been considered and modelled properly in this thesis. Also the effects that happen at pore level (nanosize level) in shales, such as very high capillary forces, adsorption and absorption are not properly modelled as they are assumed to have little impact, this should however be tested properly. Additional operational drawbacks of producing at a higher bottomhole pressure should be considered and if they impose any constrains on this method. Further more the cost term, which in this thesis are assumed to be constant, and the impact a different bottomhole pressure may have on the operation cost side should be studied.

If the above mentioned factors are considered and the method of producing at a higher bottomhole pressure still seems to be a viable option, the author recom-

mends to perform a field testing with a pilot well to confirm the results. A good candidate well should be selected based on PVT-samples that shows an initial fluid richer than the producing fluid. The PVT-samples should be taken at high enough bottomhole pressure to be able to get correct reservoir fluid characterization. The reservoir pressure must be high enough that the reservoir fluid is fairly undersaturated. The selected well should also be in an area close to other wells with field data for comparison to evaluate if the results show such improvement in oil recovery and hence net present value.

Nomenclature

$\bar{S_o}$	Average oil saturation
$\Delta\rho$	Difference between oil and gas phase densities, lb_m/ft^3
$\dot{n}$	Molar flow rate, moles/day
γ_g	Gas specific gravity
λ_g	Mobility of gas, mD/cp
λ_o	Mobility of oil, mD/cp
μ	Viscosity, cp
ϕ	Rock porosity
ρ_g	Gas density, lb_m/ft^3
σ	Interfacial tension, dynes/cm
σ_H	Largest horizontal stress, psia
σ_v	Vertical stress, psia
τ	Optimum time to change from high to low p_{wf}, days
B_g	Gas formation volume factor, ft^3/scf
B_o	Oil formation volume factor, bbl/stb
C	Cost term, USD
c_t	Total compressibility, 1/psia
CF	Cash flow
D	Wellbore diameter, inches

d_f	Discount factor
f	Fractional flow
G_p	Gas price, USD/Mscf
h	Height, ft
$IGIP$	Initial solution gas in place, scf
$IOIP$	Initial solution gas in place, stb
k	Permeability, mD
k_i	Effective permeability of phase i, mD
k_{rg}	Relative permeability of gas
$k_{rg}(S_{or}, S_{wc})$	Gas relative permeability to gas at residual oil saturation connate water saturation
k_{ri}	Relative permeability of phase i
$k_{rog}(S_{wc})$	Oil relative permeability to gas at connate water saturation
k_{ro}	Relative permeability of oil
M	Mobility ratio
$m(p)$	Pseudopressure, psia^2/cp
$m(p_i)$	Pseudopressure of initial reservoir pressure, psia^2/cp
$m(p_{wf})$	Pseudopressure of flowing bottomhole pressure, psia^2/cp
N	Number of fractures
n_g	Gas relative permeability exponent
n_{og}	Oil relative permeability exponent
NPV	Net present value, million USD
NPV_D	Dimensionless net present value
O_p	Gas price, USD/Mscf
$P.V.$	Pore volume
p_b	Bubblepoint pressure, psia
p_d	Dewpoint pressure, psia
p_f	Pore pressure, psia

p_i	Initial reservoir pressure, psia
p_t	Tubinghead pressure, psia
p_w^{frac}	Fracturing pressure of the well, psia
p_{ref}	Reference pressure, psia
p_R	Average reservoir pressure,psia
p_{sat}	Saturation pressure, psia
p_{sc}	Standard condition pressure, 14.7 psia
p_{wf}	Flowing bottomhole pressure, psia
q_D	Dimensionless rate
Q_g	Cumulative gas production, MMscf
q_g	Gas rate at standard conditions, scf/d or Mscf/d
Q_o	Cumulative oil production, Mstb
q_o	Oil rate at standard conditions, stb/d
q_o	Oil rate, stb/d
q_{min}	Minimum gas rate to lift, Mscf/d
R	Gas-oil ratio, scf/stb
r_e	Drainage radius, ft
r_p	producing oil-gas ratio, stb/MMscf
$r_s(p_{wf})$	Solution oil-gas ratio at p_{wf}, stb/MMscf
r_w	Wellbore radius, ft
R_{gas}	Universal gas constant
R_p	Producing gas-oil ratio, scf/stb
R_{si}	Initial solution gas-oil ratio, scf/stb
r_{si}	Initial oil-gas ratio, stb/MMscf
RF_g	Recovery factor of Gas
RF_o	Recovery factor of Oil
S	Hydrostatic term
s	Skin factor

S_g	Gas saturation
S_o	Oil saturation
S_{gc}	Critical gas saturation
S_{org}	Residual oil saturation to gas
S_{wc}	Connate water saturation
T	Temperature, °R
t	Time, days
T_0	Tensile strength, psia
t_D	Dimensionless time
T_{sc}	Standard condition temperature, 520 °R
TVD	True vertical depth, ft
V_o	Oil Volume, stb
$V_{\bar{g}}$	Gas volume at standard condtions, scf or MMscf
$V_{\bar{o}}$	Oil volume at standard condtions, stb
V_{roCCE}	Oil relative volume during a constant composition expansion test
x	Distance from fracture to the point where where $p = p_d$, ft
x_f	Fracture half-length, ft
y_e	Distance from fracture to outer boundary, ft
Z	Z factor
z	Wellstream composition

Bibliography

R. Aguilera. Flow Units: From Conventional to Tight Gas to Shale Gas. *SPE 132845*, 2010.

R. Aguilera. Flow Units: From Conventional to Tight Gas to Shale Gas to Shale Oil Reservoirs. *SPE 165360*, 2013.

J.D. Arthur, B. Bohm, and M. Layne. Hydraulic Fracturing Considerations for Natural Gas Wells of the Marcellus Shale, 2008. URL `http://www.dec.ny.gov/docs/materials_minerals_pdf/GWPCMarcellus.pdf`. Accessed May 2013.

K.R. Bruner and R. Smosna. A Comparative Study of the Mississippian Barnett Shale, Forth Worth Basin and Devonian Marcellus Shale, Appalachian Basin. Technical report, U.S. Department of Energy, 2011.

Coats Engineering, Inc. SENSOR Manual.

Coats Engineering, Inc. SENSOR Reservoir Simulator, 2013.

Eagle Ford Information, April 2013. URL `www.rrc.state.tx.us/eagleford/`. Accessed April 2013.

Eagleford Shale Geology. URL `http://eaglefordshale.com/geology/`. Accessed May 2013.

Nnaemeka Ezekwe. *Petroleum Reservoir Engineering Practice*. Prentice Hall, 2010.

M.D. Fetkovich, E.T. Guerrero, M.J. Fetkovich, and L.K. Thomas. Oil and Gas Relative Permeabilities Determined from Rate-Time Performance Data. *SPE 15431*, 1986.

M.J.. Fetkovich. Multipoint Testing of Gas Wells. 1975.

Ø. Fevang and C. H. Whitson. Modeling Gas Condensate Well Deliverability. *SPE 30714*, 1995.

E. Fjær, R.M. Holt, P. Horsrud, A.M. Raaen, and R. Risnes. *Petroleum Related Rock Mechanics 2nd Edition.* Elsevier, 2008.

J.L. Gidley, S.A. Holditch, D.E. Nierode, and R.W. Veatch Jr. *Recent Advances In Hydraulic Fracturing.* SPE Monograph Volume 12, 1989.

Henry Hub Natural Gas Spot Price, 2012. URL `http://www.eia.gov/naturalgas/weekly/`.

A. Holme. Modeling of Ultra-Tight Single Matrix Block. *Semester Project, NTNU*, 2012.

J.A. Jackson. Glossary of Geology. *American Geological Institute*, 1997.

D.M. Jarvie, R.J. Hill, T.E. Ruble, and R.M. Pollastro. Unconventional shale-gas systems: The Mississippian Barnett Shale of north-central Texas as one model for thermogenic shale-gas assessment. *The American Association of Petroleum Geologists Bulletin*, 91:475–499, 2007.

W.D McCain Jr. Revised Gas-Oil Ratio Criteria Key Indicators of Reservoir Fluid Type. *Petroleum Engineer International*, 1994.

W.D McCain Jr. and R.A Alexander. Sampling Gas Condensate Wells. *SPE 19729*, 1992.

Petrostreamz. Pipe-it, 2013. URL `http://petrostreamz.com/`.

Y. Tian and W.B. Ayers. Barnett Shale (Mississippian), Forth Worth Basin, Texas: Regional Varations in Gas and Oil Production and Reservoir Properties. *SPE 137766*, 2010.

Y. Tian, W.B. Ayers, and D. McCain Jr. The Eagle Ford Shale Play, South Texas: Regional Variations in Fluid Types, Hydrocarbon Production and Reservoir Properties. *IPTC 16808*, 2013.

R.G. Turner, M.G. Hubbard, and A.E. Dukler. Analysis and Prediction of Minimum Flow Rate for the Continuous Removal of Liquids from Gas Wells. *Journal of Petroleum Technology*, Volume 21, Number 11, 1969.

U.S. Energy Information Administration. URL `http://www.eia.gov/oil_gas/rpd/shale_gas.pdf`.

U.S. Energy Information Administration. Annual Energy Outlook 2012 with Projections to 2035. 2012.

U.S. Energy Information Administration. Frequently asked questions, 2013. URL `http://www.eia.gov/tools/faqs/faq.cfm?id=45&t=8`. Accessed April 2013.

J.D. Walls, E. Diaz, N. Derzhi, A. Grader, J. Dvorkin, S. Arredondo, G. Carpio, and S.W. Sinclar. Eagle Ford Shale Reservoir Properties from Digital Rock Physics. *Recovery - 2011 CSPG CSEG CWLS Convention*, 2011.

J. Wang and Y. Liu. Well Performance Modeling in Eagle Ford Shale Oil Reservoir. *SPE 144427*, 2011.

R.A. Wattenbarger, A.H. El-Banbi, and J.B. Villegas, M.E. Maggard. Production Analysis of Linear Flow Into Fractured Tight Gas Wells. *SPE 39931*, 1998.

C. H. Whitson and M.R. Brule. *Phase Behavior*. SPE, 2000.

C. H. Whitson and S. Sunjerga. PVT in Liquid-Rich Shale Reservoirs. *SPE 155499*, 2012.

Appendices

Unit Conversion

Table 1: Unit Conversion Table

	Field			SI			Other	
Pressure	1	psia	=	6895	Pa	=	0.0690	bar
Flow Rate	1	Mscf/d	=	3.277E-04	m3/s	=	28.317	m3/d
Flow Rate	1	stb/d	=	1.800E-06	m3/s	=	0.1590	m3/d
Length	1	ft	=	0.3048	m3/s			
Mass	1	lb	=	0.4536	kg			
Temperature	1	R	=	5/9	K			

EOS Data

Table 2: Base case gas condensate composition. p_d**=3800 psia** $r_{si} = 100 stb/MMscf$

Fluid Composition	
Component	Mole fraction
H2S	0.00%
N2	1.62%
CO2	6.82%
C1	67.61%
C2	8.42%
C3	4.70%
I-C4	0.63%
N-C4	1.77%
I-C5	0.60%
N-C5	0.71%
C6	0.80%
C7	1.65%
C8	1.73%
C9	1.04%
C10	0.659%
C11	0.425%
C12	0.276%
C13	0.179%
C14	0.118%
C15	0.079%
C16	0.052%
C17	0.035%
C18	0.024%
C19	0.016%
C20	0.0109%
C21	0.0074%
C22	0.0051%
C23	0.0035%
C24	0.0024%
C25	0.0017%
C26+	0.0032%

Table 3: SRK Equation of State Data

	M	Tc R	Pc psia	Zcrit	Shift-f	ω	Parachor	Omega-A	Omega-B
H2S	34	672	1300	0.283	0.102	0.090	80.1	0.427	0.087
N2	28	227	493	0.292	-0.001	0.037	59.1	0.427	0.087
CO2	44	547	1070	0.274	0.217	0.225	80.0	0.427	0.087
C1	16	343	667	0.286	-0.002	0.011	71.0	0.427	0.087
C2	30	550	707	0.279	0.059	0.099	111.0	0.427	0.087
C3	44	666	616	0.276	0.091	0.152	151.0	0.427	0.087
I-C4	58	734	528	0.282	0.110	0.186	188.8	0.427	0.087
N-C4	58	765	551	0.274	0.110	0.200	191.0	0.427	0.087
I-C5	72	829	490	0.272	0.098	0.229	227.4	0.427	0.087
N-C5	72	845	489	0.268	0.119	0.252	231.0	0.427	0.087
C6	82	924	490	0.249	0.134	0.238	232.8	0.427	0.087
C7	96	991	454	0.267	0.144	0.274	265.5	0.427	0.087
C8	109	1043	421	0.265	0.153	0.311	296.3	0.427	0.087
C9	122	1094	389	0.261	0.170	0.351	327.9	0.427	0.087
C10	135	1138	360	0.258	0.187	0.391	358.9	0.427	0.087
C11	148	1178	336	0.255	0.202	0.431	389.7	0.427	0.087
C12	161	1215	314	0.252	0.217	0.470	420.3	0.427	0.087
C13	173	1249	295	0.250	0.231	0.508	450.7	0.427	0.087
C14	186	1280	278	0.247	0.244	0.546	480.8	0.427	0.087
C15	198	1309	263	0.245	0.256	0.583	510.6	0.427	0.087
C16	211	1336	250	0.243	0.266	0.620	540.2	0.427	0.087
C17	223	1361	238	0.242	0.277	0.655	569.6	0.427	0.087
C18	235	1384	227	0.240	0.286	0.691	598.6	0.427	0.087
C19	247	1406	218	0.239	0.294	0.725	627.4	0.427	0.087
C20	259	1427	209	0.238	0.302	0.759	655.9	0.427	0.087
C21	270	1447	201	0.237	0.309	0.792	684.2	0.427	0.087
C22	282	1465	194	0.237	0.316	0.824	712.1	0.427	0.087
C23	294	1483	187	0.236	0.322	0.856	739.9	0.427	0.087
C24	305	1500	181	0.236	0.327	0.887	767.3	0.427	0.087
C25	316	1516	175	0.235	0.332	0.918	794.5	0.427	0.087
C26+	412	1631	141	0.237	0.360	1.162	1024.3	0.427	0.087

Table 4: Binary Interaction Parameters

	H2S	N2	CO2	C1
H2S	0	0	0	0.08
N2	0	0	0	0.02
CO2	0	0	0	0.12
C1	0.08	0.02	0.12	0
C2	0.07	0.06	0.12	0
C3	0.07	0.08	0.12	0
I-C4	0.06	0.08	0.12	0
N-C4	0.06	0.08	0.12	0
I-C5	0.06	0.08	0.12	0
N-C5	0.06	0.08	0.12	0
C6	0.05	0.08	0.12	0
C7	0.03	0.08	0.1	0.03
C8	0.03	0.08	0.1	0.03
C9	0.03	0.08	0.1	0.03
C10	0.03	0.08	0.1	0.04
C11	0.03	0.08	0.1	0.04
C12	0.03	0.08	0.1	0.04
C13	0.03	0.08	0.1	0.05
C14	0.03	0.08	0.1	0.05
C15	0.03	0.08	0.1	0.05
C16	0.03	0.08	0.1	0.06
C17	0.03	0.08	0.1	0.06
C18	0.03	0.08	0.1	0.06
C19	0.03	0.08	0.1	0.06
C20	0.03	0.08	0.1	0.06
C21	0.03	0.08	0.1	0.07
C22	0.03	0.08	0.1	0.07
C23	0.03	0.08	0.1	0.07
C24	0.03	0.08	0.1	0.07
C25	0.03	0.08	0.1	0.07
C26+	0.03	0.08	0.1	0.08

Grid Dimensions

Table 5: Grid Dimensions in the x-direction

i	Δ X	i	Δ X	i	Δ X	i	Δ X
1	19.6201	21	0.34913	41	0.009295	61	0.522347
2	16.0404	22	0.285432	42	0.011369	62	0.638918
3	13.1139	23	0.233355	43	0.013906	63	0.781503
4	10.7212	24	0.190779	44	0.01701	64	0.955909
5	8.76515	25	0.155971	45	0.020806	65	1.16924
6	7.16595	26	0.127514	46	0.025449	66	1.43017
7	5.85852	27	0.104249	47	0.031129	67	1.74934
8	4.78963	28	0.085229	48	0.038075	68	2.13973
9	3.91576	29	0.069679	49	0.046573	69	2.61725
10	3.20133	30	0.056966	50	0.056966	70	3.20133
11	2.61725	31	0.046573	51	0.069679	71	3.91576
12	2.13973	32	0.038075	52	0.085229	72	4.78963
13	1.74934	33	0.031129	53	0.104249	73	5.85852
14	1.43017	34	0.025449	54	0.127514	74	7.16595
15	1.16924	35	0.020806	55	0.155971	75	8.76515
16	0.955909	36	0.01701	56	0.190779	76	10.7212
17	0.781503	37	0.013906	57	0.233355	77	13.1139
18	0.638918	38	0.011369	58	0.285432	78	16.0404
19	0.522347	39	0.009295	59	0.34913	79	19.6201
20	0.427045	40	0.0833	60	0.427045		

Table 6: Grid Dimensions in the y-direction

j	Δ Y	j	Δ Y	j	Δ Y
1	33.1847	21	0.224119	41	2.09838
2	25.8473	22	0.174565	42	3.11512
3	20.1322	23	0.135967	43	4.62451
4	15.6808	24	0.105904	44	6.86526
5	12.2137	25	0.082487	45	10.1917
6	9.51312	26	0.064249	46	15.13
7	7.40969	27	0.050043	47	22.4611
8	5.77134	28	0.038978	48	33.3443
9	4.49525	29	0.03036	49	49.5009
10	3.50131	30	0.023647	50	73.4859
11	2.72715	31	0.040362		
12	2.12415	32	0.059919		
13	1.65448	33	0.088952		
14	1.28866	34	0.132052		
15	1.00373	35	0.196036		
16	0.781796	36	0.291023		
17	0.608935	37	0.432035		
18	0.474294	38	0.641372		
19	0.369424	39	0.952141		
20	0.287741	40	1.41349		

Dimensionless Variables

$$q_D = \frac{141.2 q \mu B}{kh(p_i - p_{wf})} \tag{1}$$

$$t_D = \frac{0.00633 kt}{\phi \mu c_t r_w^2} \tag{2}$$

SENSOR Data Input File

Base Case 2D Gas Condensate Data File

```
TITLE
 Sensor Data Set
 Ultra-tight liquid-rich well performance.
 Single fracture segment
 2D Model
 June 2013
ENDTITLE

GRID 79 50 1
PCMULT2 0. 0.
RUN
CPU
IMPLICIT



MAPSPRINT 1 P SO SW KX
MAPSFILE P SW SO SG

C    Bwi cw     denw  visw  cr      pref
MISC 1   3.0E-6 62.4  0.5   4.0E-6  6000

C ------------------------------------------------------------------------------------
C Including grid definition created by SensorGrid
C ------------------------------------------------------------------------------------
C ----------------------------------
C I_CELLS          79
C J_CELLS          50
C K_CELLS          1
C DEPTH            6500
C SYM_ELEMENTS     2
C FRAC_AREA        37500
C ----------------------------------

C ------------------------------------------------------------------------------------
C Cell width along wellbore
C ------------------------------------------------------------------------------------
DELX XVAR
19.6201 16.0404 13.1139 10.7212 8.76515 7.16595 5.85852 4.78963
3.91576 3.20133 2.61725 2.13973 1.74934 1.43017  1.16924
0.955909 0.781503 0.638918 0.522347 0.427045 0.34913 0.285432
0.233355 0.190779 0.155971 0.127514 0.104249 0.0852291
0.069679 0.0569661 0.0465726 0.0380754 0.0311286 0.0254492
0.020806 0.0170099 0.0139064 0.0113692 0.0092949
0.0833
0.0092949 0.0113692 0.0139064 0.0170099 0.020806 0.0254492
0.0311286 0.0380754 0.0465726 0.0569661 0.069679 0.0852291
0.104249 0.127514 0.155971 0.190779 0.233355 0.285432 0.34913
0.427045 0.522347 0.638918 0.781503  0.955909 1.16924
1.43017 1.74934 2.13973 2.61725 3.20133 3.91576
4.78963 5.85852 7.16595 8.76515 10.7212 13.1139 16.0404 19.6201

C ------------------------------------------------------------------------------------
C Cell width away from wellbore
C ------------------------------------------------------------------------------------
DELY YVAR
```

```
33.1847 25.8473 20.1322 15.6808 12.2137 9.51312 7.40969 5.77134 4.49525
3.50131 2.72715 2.12415 1.65448 1.28866 1.00373 0.781796 0.608935
0.474294 0.369424 0.287741 0.224119 0.174565 0.135967 0.105904
0.0824874 0.0642487 0.0500428 0.0389779 0.0303596 0.0236468 0.040362
0.0599188 0.0889518 0.132052 0.196036 0.291023 0.432035
0.641372 0.952141 1.41349 2.09838 3.11512 4.62451 6.86526
10.1917 15.13 22.4611 33.3443 49.5009 73.4859


C ----------------------------------------------------------------------------------------
C Porosity
C ----------------------------------------------------------------------------------------
POROS CON
 0.05

MOD
40 40 1 30 1 1 = 0.0389574


C ----------------------------------------------------------------------------------------
C Rocktype (for relperm curves)
C ----------------------------------------------------------------------------------------
ROCKTYPE CON
 1

MOD
40 40 1 30 1 1 = 2

C ----------------------------------------------------------------------------------------
C Permeability
C ----------------------------------------------------------------------------------------
KX CON
 0.0001

MOD
40 40 1 30 1 1 = 12004.8

KY EQUALS KX
KZ EQUALS KX

C ----------------------------------------------------------------------------------------
C Depth
C ----------------------------------------------------------------------------------------
DEPTH CON
 6500

C ----------------------------------------------------------------------------------------
C Thickness
C ----------------------------------------------------------------------------------------
THICKNESS CON
 250



C ----------------------------------------------------------------------------------------
C Relperm
C ----------------------------------------------------------------------------------------

KRANALYTICAL 1    ! For matrix
 0.2 0.2 0.2 0.1 ! Swc Sorw Sorg Sgc
 1 1 1           ! krw(Sorw) krg(Swc) kro(Swc)
 2 2 2 2  ! nw now ng nog
 -10 10 1. PCGO

 KRANALYTICAL 2   ! For fractures
 0.20 0.2 0.2 0.1 ! Swc Sorw Sorg Sgc
 1 1 1            ! krw(Sorw) krg(Swc) kro(Swc)
 1 1 1 1
 -10 10 1. PCGO   ! pcgo_frac


C ----------------------------------------------------------------------------------------
C Including black oil table
C ----------------------------------------------------------------------------------------

BLACKOIL    1     29    30    SRK
PRESSURES 14.7        200        400        600        800        1000
1200        1400        1600        1800        2000        2200        2400
2600        2800        3000        3200        3400        3600        3800
4000        4400        4800        5200        5600        6000        7000
8000        9000        10000
```

```
RESERVOIR FLUID
C -- Initial Reservoir Composition
C -- Initial Reservoir Composition
0.00000000
0.00980125
0.06660742
0.52348708
0.09132449
0.06119169
0.00907845
0.02705838
0.01019258
0.01256173
0.01586423
0.03728877
0.04271827
0.02804334
0.01942073
0.01348196
0.00938946
0.00656252
0.00460370
0.00324175
0.00229142
0.00162588
0.00115806
0.00082799
0.00059423
0.00042806
0.00030949
0.00022457
0.00016352
0.00011948
0.00033948

INJECTION GAS EQUILIBRIUM

SEPARATOR
440   104
14.70 60.0

ENDBLACKOIL

C ======================================================================
C Fluid Properties
C ======================================================================
PVTEOS SRK
135    ! Reservoir temperature (deg F)

CPT         MW          TC          PC          ZCRIT       SHIFT       AC          PCHOR       OMEGA       OMEGB
   H2S      34.082      672.12      1300        0.28292     0.10153     0.09        80.1        0.42748     0.08664
   N2       28.014      227.16      492.84      0.29178     -0.0009     0.037       59.1        0.42748     0.08664
   CO2      44.01       547.42      1069.5      0.27433     0.21749     0.225       80          0.42748     0.08664
   C1       16.043      343.01      667.03      0.2862      -0.00247    0.011       71          0.42748     0.08664
   C2       30.07       549.58      706.62      0.27924     0.05894     0.099       111         0.42748     0.08664
   C3       44.097      665.69      616.12      0.2763      0.09075     0.152       151         0.42748     0.08664
   I-C4     58.123      734.13      527.94      0.28199     0.10952     0.186       188.8       0.42748     0.08664
   N-C4     58.123      765.22      550.56      0.27385     0.11028     0.2         191         0.42748     0.08664
   I-C5     72.15       828.7       490.37      0.27231     0.09773     0.229       227.4       0.42748     0.08664
   N-C5     72.15       845.46      488.78      0.26837     0.11947     0.252       231         0.42748     0.08664
   C6       82.422      924.04      489.98      0.24891     0.13417     0.23825     232.81      0.42748     0.08664
   C7       96.053      990.58      454.18      0.26708     0.14355     0.27411     265.53      0.42748     0.08664
   C8       108.89      1043.4      421.37      0.26505     0.15263     0.31051     296.33      0.42748     0.08664
   C9       122.04      1093.5      388.54      0.26121     0.17011     0.35127     327.89      0.42748     0.08664
   C10      134.96      1138        360.26      0.25783     0.18663     0.39131     358.9       0.42748     0.08664
   C11      147.8       1178.2      335.58      0.25479     0.20229     0.43091     389.72      0.42748     0.08664
   C12      160.55      1214.9      313.96      0.25202     0.21703     0.46995     420.31      0.42748     0.08664
   C13      173.19      1248.7      294.94      0.24952     0.2308      0.50837     450.67      0.42748     0.08664
   C14      185.74      1279.8      278.13      0.24726     0.24362     0.54615     480.77      0.42748     0.08664
   C15      198.18      1308.7      263.19      0.24523     0.25551     0.58326     510.63      0.42748     0.08664
   C16      210.51      1335.5      249.88      0.24342     0.26648     0.61969     540.22      0.42748     0.08664
   C17      222.73      1360.6      237.95      0.24182     0.27659     0.65545     569.55      0.42748     0.08664
   C18      234.83      1384.1      227.23      0.24043     0.28589     0.69052     598.6       0.42748     0.08664
   C19      246.83      1406.2      217.56      0.23921     0.29442     0.72492     627.39      0.42748     0.08664
   C20      258.71      1427        208.81      0.23817     0.30224     0.75865     655.91      0.42748     0.08664
   C21      270.48      1446.7      200.85      0.2373      0.3094      0.79172     684.16      0.42748     0.08664
   C22      282.14      1465.3      193.61      0.23658     0.31594     0.82413     712.14      0.42748     0.08664
   C23      293.69      1483        186.98      0.236       0.32191     0.8559      739.86      0.42748     0.08664
   C24      305.13      1499.8      180.91      0.23556     0.32736     0.88704     767.32      0.42748     0.08664
   C25      316.47      1515.8      175.33      0.23524     0.33233     0.91755     794.52      0.42748     0.08664
   C26+     412.23      1631.4      140.76      0.23657     0.36046     1.1619      1024.3      0.42748     0.08664
```

```
BIN
0       0       0.08    0.07    0.07    0.06    0.06    0.06    0.06
0.05    0.03    0.03    0.03    0.03    0.03    0.03    0.03    0.03
0.03    0.03    0.03    0.03    0.03    0.03    0.03    0.03    0.03
0.03    0.03    0.03
0       0.02    0.06    0.08    0.08    0.08    0.08    0.08    0.08
0.08    0.08    0.08    0.08    0.08    0.08    0.08    0.08    0.08
0.08    0.08    0.08    0.08    0.08    0.08    0.08    0.08    0.08
0.08    0.08
0.12    0.12    0.12    0.12    0.12    0.12    0.12    0.12    0.1
0.1     0.1     0.1     0.1     0.1     0.1     0.1     0.1     0.1
0.1     0.1     0.1     0.1     0.1     0.1     0.1     0.1     0.1
0.1
0       0       0       0       0       0       0       0.02586 0.02979
0.03393 0.0378  0.04143 0.04483 0.04801 0.05096 0.05371 0.05627 0.05864
0.06085 0.0629  0.06481 0.06659 0.06825 0.0698  0.07124 0.0726  0.0815
0       0       0       0       0       0       0       0       0
0       0       0       0       0       0       0       0       0
0       0       0       0       0       0       0       0
0       0       0       0       0       0       0       0       0
0       0       0       0       0       0       0       0       0
0       0       0       0       0       0       0
0       0       0       0       0       0       0       0       0
0       0       0       0       0       0       0       0       0
0       0       0       0       0       0
0       0       0       0       0       0       0       0       0
0       0       0       0       0       0       0       0       0
0       0       0       0       0
0       0       0       0       0       0       0       0       0
0       0       0       0       0       0       0       0       0
0       0       0       0
0       0       0       0       0       0       0       0       0
0       0       0       0       0       0       0       0       0
0       0       0
0       0       0       0       0       0       0       0       0
0       0       0       0       0       0       0       0       0
0       0
0       0       0       0       0       0       0       0       0
0       0       0       0       0       0       0       0       0
0
0       0       0       0       0       0       0       0       0
0       0       0       0       0       0       0       0       0
0       0       0       0       0       0       0       0       0
0       0       0       0       0       0       0       0
0       0       0       0       0       0       0       0       0
0       0       0       0       0       0       0
0       0       0       0       0       0       0       0       0
0       0       0       0       0       0
0       0       0       0       0       0       0       0       0
0       0       0       0       0
0       0       0       0       0       0       0       0       0
0       0       0       0
0       0       0       0       0       0       0       0       0
0       0       0
0       0       0       0       0       0       0       0       0
0       0
0       0       0       0       0       0       0       0       0
0
0       0       0       0       0       0       0       0       0
0       0       0       0       0       0       0       0
0       0       0       0       0       0       0
0       0       0       0       0       0
0       0       0       0       0
0       0       0       0
0       0       0
0       0
0

C ------------------------------------------------------------------------------------------
C Initialize
C ------------------------------------------------------------------------------------------
INITIAL


DEPTH GOR
6625 10000


GOC 6625
PINIT 6000
```

```
ENDINIT
C ------------------------------------------------------------------------------------------
C Include recurrent data generated by SensorGrid (perforations and TZ modifiers)
C ------------------------------------------------------------------------------------------
C ----------------------------------
C Trans. modification to fractures
C ----------------------------------
MODIFY TX 1.0
 39 39 30 30 1 1 * 1
 40 40 30 30 1 1 * 1


C ----------------------------------
C Define Wells
C ----------------------------------
WELL
        I J  K   PI
 PROD   40 1 1   100
 INJ    40 1 1   100


C ------------------------------------------------------------------------------------------
C Include tubinghead table
C ------------------------------------------------------------------------------------------
C INCLUDE
C  thp.inc


BHP
 PROD 1000
 INJ  8000

SKIP
THP
 PROD 100 -2
SKIPEND

WELLTYPE
 PROD MCF
 INJ  STBWATINJ

PSM


MAPSFREQ -1
MAPSFILEFREQ 20
DTMAX 1

C ------------------------------------------------------------------------------------------
C Define rate schedules.
C ------------------------------------------------------------------------------------------

WELLTYPE
 PROD MCF
RATE
 PROD 18518.5
TIME 3650

END
```